Bulletin of Volcanology (2022) 84: 28
https://doi.org/10.1007/s00445-021-01522-8

REVIEW ARTICLE

Open-vent volcanoes fuelled by depth-integrated magma degassing

M. Edmonds[1] · **E.J. Liu**[2] · **K.V. Cashman**[3]

Received: 8 July 2021 / Accepted: 13 December 2021 / Published online: 15 February 2022

Abstract

Open-vent, persistently degassing volcanoes—such as Stromboli and Etna (Italy), Villarrica (Chile), Bagana and Manam (Papua New Guinea), Fuego and Pacaya (Guatemala) volcanoes—produce high gas fluxes and infrequent violent strombolian or 'paroxysmal' eruptions that erupt very little magma. Here we draw on examples of open-vent volcanic systems to highlight the principal characteristics of their degassing regimes and develop a generic model to explain open-vent degassing in both high and low viscosity magmas and across a range of tectonic settings. Importantly, gas fluxes from open-vent volcanoes are far higher than can be supplied by erupting magma and independent migration of exsolved volatiles is integral to the dynamics of such systems. The composition of volcanic gases emitted from open-vent volcanoes is consistent with its derivation from magma stored over a range of crustal depths that in general requires contributions from both magma decompression (magma ascent and/or convection) and iso- and polybaric second boiling processes. Prolonged crystallisation of water-rich basalts in crustal reservoirs produces a segregated exsolved hydrous volatile phase that may flux through overlying shallow magma reservoirs, modulating heat flux and generating overpressure in the shallow conduit. Small fraction water-rich melts generated in the lower and mid-crust may play an important role in advecting volatiles to subvolcanic reservoirs. Excessive gas fluxes at the surface are linked to extensive intrusive magmatic activity and endogenous crustal growth, aided in many cases by extensional tectonics in the crust, which may control the longevity and activity of open-vent volcanoes. There is emerging abundant geophysical evidence for the existence of a segregated exsolved magmatic volatile phase in magma storage regions in the crust. Here we provide a conceptual picture of gas-dominated volcanoes driven by magmatic intrusion and degassing throughout the crust.

Keywords Open-vent volcanoes · Depth-integrated magma degassing · Gas-dominated volcanoes

Introduction

Open-vent volcanoes are characterised by their persistent outgassing and mildly explosive activity between major eruptions (Andres and Kasgnoc 1998; Francis et al. 1993; Rose et al. 2013; Vergniolle and Métrich 2021). Many are well studied because persistent low-level activity allows access and collection of extended time series of monitoring data. Open-vent volcanoes are found in all tectonic settings and are associated with a range of magma compositions and bulk viscosities (some examples—not an exhaustive list—are shown in Fig. 1 and Table S1). Open-vent volcanoes may be active over millennia—for example Masaya, Nicaragua (Stix 2007), Stromboli, Italy (Allard et al. 1994), Etna, Italy (Allard 1997), Villarrica, Chile (Witter et al. 2004), Yasur Volcano, Vanuatu (Métrich et al. 2011) and Erebus, Antarctica (Oppenheimer et al. 2011)—or years to decades, such as Soufrière Hills, Montserrat (Christopher et al. 2010) and Fuego (Lyons et al. 2010) and Santiaguito, Guatemala (Holland et al. 2011).

Volcanoes that transition from being 'open vent' to 'closed vent' over years to decades timescales may be classified as 'persistently restless'. For example, Telica Volcano, Nicaragua, transitions between a 'weak seal' and a 'destabilised' state, which may produce phreatomagmatic eruptions

Editorial responsibility: N. Métrich

This paper constitutes part of a topical collection: Open-vent volcanoes

✉ M. Edmonds
me201@cam.ac.uk

[1] Department of Earth Sciences, University of Cambridge, Downing St, Cambridge CB2 3EQ, UK

[2] Earth Sciences, University College London, 5 Gower Place, London WC1E 6BS, UK

[3] Earth Sciences, University of Bristol, Wills Memorial Building, Bristol BS8 1RJ, UK

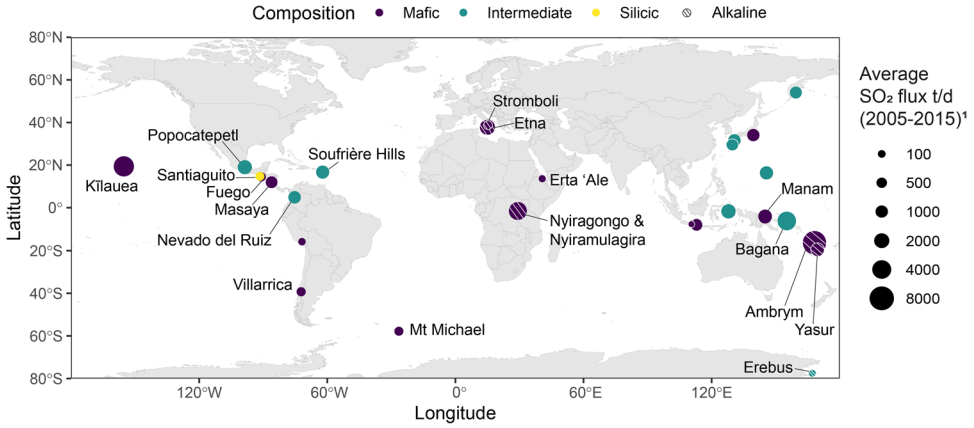

Fig. 1 Global distribution of open-vent volcanoes, listed in Supplementary table S1, encompassing a broad range of magma compositions and tectonic settings. Superscript 1: Average SO_2 flux (2005–2015) from Carn et al. (2017)

(Rodgers et al. 2015; Roman et al. 2019). Long-dormant volcanoes may also convert to open-system behaviour when they reactivate. Reactivation may initiate explosively, as at Santa María volcano in Guatemala (now the location of the open-vent effusion of the Santiaguito flank volcano) (Lamb et al. 2019), or effusively, as at Soufrière Hills volcano, Montserrat (Wadge et al. 2014). Following the initiation of activity in 1995, Soufrière Hills has outgassed continuously for more than 25 years at the time of writing, despite not being in a state of eruption for much of that time (Christopher et al. 2015).

Eruptions of open-vent volcanoes are typically gas-rich and may be highly hazardous. The nature of the eruptive activity varies with magma composition. Mafic stratovolcanoes exhibiting open-vent behaviour—such as the archetypal Stromboli volcano, Italy—exhibit frequent strombolian eruptions punctuated by large violent explosions, or 'paroxysms' (Bertagnini et al. 2011; Métrich et al. 2005; Rosi et al. 2006). Persistent degassing from mafic lava lakes may persist over decades or longer with accompanying strombolian explosions and/or lake overflows or draining events (e.g. Ambrym, Vanuatu; Erta Ale, Ethiopia; Masaya, Nicaragua) (Bouche et al. 2010; Lev et al. 2019; Moussallam et al. 2021). Open-system behaviour in more evolved systems is typically accompanied by episodic explosive activity (typically vulcanian or violent strombolian in style depending on the melt composition; Cashman and Sparks 2013), effusion of viscous lava flows and domes and/or gas venting episodes (Edmonds and Herd 2007). The over-arching characteristics of open-vent activity in all settings, however, are that the outgassing flux of volatiles far exceeds the volatiles that can be supplied from degassing of erupted magma and that high levels of outgassing from a central vent continues between eruptions (Andres et al. 1991). Open-vent volcanoes may therefore be thought of as predominantly gas emitters, with the magma that is supplying the outgassing accumulating endogenously in the crust beneath (Allard 1997; Anderson 1975; Francis et al. 1993; Giggenbach 1992; Giggenbach 1996). Where in the crust the magma accumulates is, however, an open question.

It has also been shown that open-vent volcanoes are the most prodigious volcanic outgassers of volatiles into the atmosphere, worldwide (Andres and Kasgnoc 1998; Carn et al. 2016). Additionally, extensive records of the outgassing fluxes of open-vent volcanoes from many decades of in situ measurements (Arellano et al. 2021; Carn et al. 2016; Carn et al. 2017; Fioletov et al. 2016) show that outgassing between eruptions dominates the volcanic gas budget (Allard 1997; Carn et al. 2016; Carn et al. 2017). Indeed, satellite-based global observations of SO_2 flux confirms that persistent, or passive, degassing accounts for ~ 90% of the global outgassing sulphur flux from volcanoes (Carn et al. 2016; Carn et al. 2017) and that most of the top 20 volcanic outgassers, as quantified from UV sensors total ozone mapping spectrometer (TOMS) and ozone mapping instrument (OMI), may be classified as 'open-vent' (Table S1; Fig. 1) (Carn et al. 2017).

Background and aims of this review

Outstanding questions related to outgassing from open-vent volcanoes

The most pressing questions surrounding the outgassing of open-vent volcanoes, and the consequent implications for both monitoring and understanding how these volcanoes work, concern the sources and mechanisms of volatile degassing. Volatiles (e.g. H_2O, CO_2) exsolve from magma upon reaching saturation in the silicate melt or by partitioning into a pre-existing exsolved phase (e.g. sulphur, chlorine) (Aiuppa et al. 2008; Candela 1997; Cashman 2004; Edmonds and Wallace 2017; Edmonds and Woods 2018; Métrich and Wallace 2008; Wallace 2005) (Fig. 2). Volatile degassing from melts occurs during decompression (sometimes called 'first boiling'; Fig. 2a);

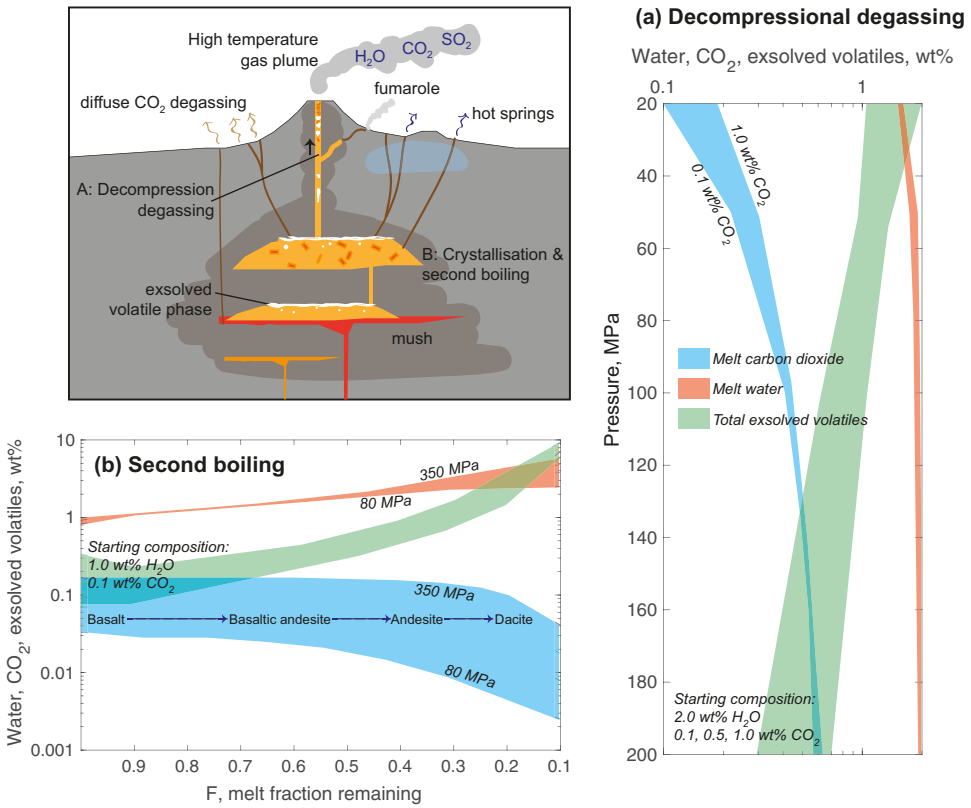

Fig. 2 Schematic illustration of a volcanic system to illustrate potential sources of outgassing volatiles. Magmas degas volatiles in response to **A** decompression during transit to the surface. The plot shows the concentrations of water (red) and carbon dioxide (blue) in a basaltic melt during decompression to the surface from a pressure of 200 MPa (modelled using MagmaSat; (Ghiorso and Gualda 2015b). The green shaded area shows the amount of exsolved volatile phase produced during degassing. In this case, the basalt has a bulk concentration of 2 wt% H_2O and a range in CO_2 concentrations from 0.1 to 1 wt%. The exsolved volatile phase thus produced may outgas to the atmosphere during eruptions. Magmas also degas in response to **B** crystallisation in magma reservoirs in the crust. Crystallisation drives up the concentrations of volatiles in the residual melt and causes the formation of a substantial exsolved volatile phase after differentiation of the magma to highly evolved compositions. In this closed system, degassing model involving crystallisation occurring at pressures of 80 to 350 MPa, a primitive basalt begins (at F = 1) with 1 wt% H_2O and 0.1 wt% CO_2. After 50% crystallisation, the magma has reached basaltic andesite composition and, after 80%, approximately dacite composition

this drives undercooling and crystallisation (Cashman and Blundy 2000) and, as a result of isobaric cooling and crystallisation, second boiling in magma reservoirs in the crust (Fig. 2b). For open-vent volcanoes, where large fluxes of gases are sustained with comparatively little magma erupted (Table S1), key questions include (1) the extent to which exsolved volatiles derive from first and/or second boiling, (2) mechanisms of volatile transfer upward through the magmatic system (i.e. as an exsolved magmatic volatile phase (hereafter MVP) or retained within volatile-rich melts) and (3) the effect of the volatile transfer mechanism on resulting volcanic activity (Fig. 2).

Degassing in the volcanic conduit

A popular model to explain the high observed outgassing fluxes of water, sulphur, CO_2 and halogen species at mafic open-vent volcanoes is bimodal flow driven by convection, whereby buoyant, volatile-rich magma rises up a conduit and degasses; then, the denser, gas-free magma sinks over vertical length scales of several kilometres (Kazahaya et al. 1994; Palma et al. 2011; Shinohara 2008; Stevenson and Blake 1998) (Fig. 3a). Convective flow has been reproduced in both analogue and numerical experiments (Beckett et al. 2011; Cardoso and Woods 1999; Huppert and Hallworth 2007; Molina et al. 2012). A simple Poiseuille flow model of buoyancy-driven ascent of magma in a conduit is given by:

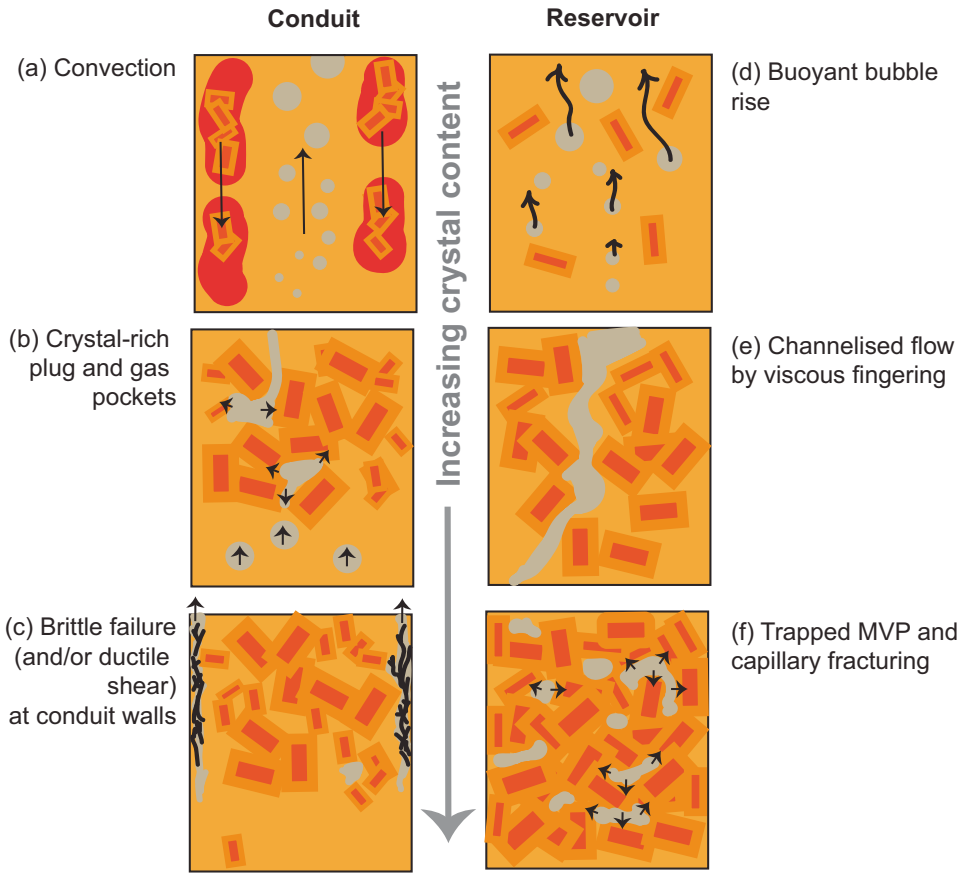

Fig. 3 Conceptual frameworks to understand the magmatic volatile phase (MVP) segregation from magmas in conduits (**a**, **b**, **c**) and in reservoirs (**d**, **e**, **f**) that may be relevant to open-vent volcanic systems. In conduits, **a** convection is driven by density differences, with volatile-rich melts ascending, vesiculating, outgassing, then sinking (Kazahaya et al. 2004; Palma et al. 2011; Shinohara et al. 1995; Stevenson and Blake 1998). Crystals are generated by degassing-induced crystallisation in degassed, sinking melts (Beckett et al. 2014). **b** For open-vent volcanoes exhibiting strombolian activity, volcanic gases may accumulate in a shallow, crystal-rich plug made up of degassed and crystallised magma (Barth et al. 2019; Belien et al. 2010; Gurioli et al. 2014; Oppenheimer et al. 2015; Suckale et al. 2016; Woitischek et al. 2020); explosions may be caused by overpressure in the gas pockets overcoming the local yield strength in the crystal pack. **c** At low confining pressures and high magma viscosities, there may be sufficient strain at the conduit walls to induce brittle failure, with gas loss along permeable channels (e.g. Santiaguito, Mount St Helens 2004-2006) (Dingwell 1996; Edmonds and Herd 2007; Gonnermann and Manga 2003; Tuffen and Dingwell 2005). In crustal magma reservoirs, it has been proposed that the MVP may segregate under different regimes depending on magma crystal content. **d** In crystal-poor melt lenses, the dominant regime may be buoyant bubble rise, the timescale for which is governed by the density difference between melt and MVP, the melt viscosity and the bubble size (Parmigiani et al. 2016). **e** In more crystal-rich mobile mushes, the MVP may rise buoyantly by viscous fingering, forming interconnected channels which may allow potentially much faster MVP segregation (Parmigiani et al. 2016). **f** In crystal-rich, melt-poor mush, the MVP may become trapped in pore spaces, becoming mobilised once a critical overpressure is reached inside the pores, which may induce capillary fracturing (Degruyter et al. 2019; Parmigiani et al. 2016)

$$Q_{ascend} = \frac{\pi \Delta \rho_{d-a} g r_a^4}{8 \mu_a}, \quad (1)$$

(Kazahaya et al. 1994) where Q_{ascend} is the volume flux of ascending magma, g is the gravitational constant, $\Delta \rho_{d-a}$ is the density difference between the bubble-rich magma at depth and the shallow degassed magma, r_a is the effective conduit radius for ascending magma and μ_a is the viscosity of ascending magma. If no magma is erupted, then Q_{ascend} must be balanced by the volume flux of descending magma minus the volume of the volatiles released to the surface (Kazahaya et al. 1994; Stevenson and Blake 1998). SO_2 fluxes of 10^2–10^3 tonnes per day (typical of many of the volcanoes highlighted in Fig. 1 and table S1), for example require magma fluxes in the conduit of ~ 1–10 m^3/s. Magma flux, in turn, is controlled by the conduit radius (assuming a cylindrical geometry) and the flow velocity, which is a function of magma viscosity and density. If the gas is transported with the magma, maintaining the same gas supply (assuming similar exsolved gas contents) requires magma with a viscosity of 10^8 Pa s to occupy a conduit approximately ten times wider than magma with a viscosity of 10^4 Pa s.

Critically, however, H_2O-rich magmas do not maintain constant viscosities as they ascend, because they undergo extensive decompression-induced degassing and consequent crystallisation (Cashman and Blundy 2000; Lipman et al. 1985; Métrich and Rutherford 1998). The addition of crystals may increase the magma viscosity by orders of magnitude (Lejeune and Richet 1995). Ultimately, it is likely that slowly-rising water-rich magmas will entirely crystallise, as observed in lava domes, and therefore, convection is unlikely. In lower viscosity magmas, changing the viscosity contrast between the down- and upwelling liquids can affect the geometry of the exchange flow (Beckett et al. 2014). It has been suggested that magma may overturn at various depths before reaching the surface (e.g. Masaya, Nicaragua; Aiuppa et al. 2018; Stix 2007). Regardless of the exact location, however, magma overturn within the shallow system requires that degassed magmas accumulate in subsurface storage regions. At Etna, Italy, for example there is evidence for endogenous accumulation of degassed magma at a rate of $22.9 \pm 13.7 \times 10^6$ m^3 $year^{-1}$ in a storage region between 3 and 10 km beneath the surface (Coppola et al. 2019); whether this magma crystallised in situ or degassed higher in the system is not known, a topic debated by a range of authors in the past (Allard 1997; Steffke et al. 2011).

Alternative models to explain the outgassing flux from open-vent volcanoes invoke the permeable flow of an exsolved volatile phase through magma in the conduit. In viscous magmas, gas flow is governed by bubble connectivity and the development of permeability. In the absence of crystals, permeability development during decompression of a hydrous melt depends on decompression rate, magma composition (viscosity) and shear (e.g. Giachetti et al. 2019; Hurwitz and Navon 1994; Lindoo et al. 2016; Okumura et al. 2006, 2008, 2013). Experimentally determined vesicularity thresholds for permeability development vary from ~ 30 to 80%, depending on the deformation regime (Okumura et al. 2008). Experimental data suggest that efficient, channelised gas flow may occur at depths of a few kilometres through rhyolite melt containing 5 wt% H_2O when subject to a shear strain > 8 (Okumura et al. 2008). The addition of crystals may substantially reduce the percolation threshold for system-scale connectivity during vesiculation and may promote efficient gas loss from conduits even at low gas fractions (Colombier et al. 2020; Collombet et al. 2021; deGraffenried et al. 2019; Lindoo et al. 2017; Fig. 3b). Degassing-induced rheological changes in shallow conduit magma may promote brittle fracturing at the conduit walls, providing transient, highly permeable pathways for gas loss (Gaunt et al. 2014; Gonnermann and Manga 2003; Rust et al. 2004; Tuffen and Dingwell 2005) (Fig. 3c) and generating low-frequency seismicity (Iverson 2008; Neuberg et al. 2006).

In crystal-rich magmas, gas may be trapped in pore spaces between crystals, where it may accumulate until the overpressure generated overcomes the local yield strength of the crystal framework (Belien et al. 2010; Oppenheimer et al. 2015); this presents a mechanism by which gases may accumulate in crystal-rich plugs and subsequently trigger strombolian eruptions (Oppenheimer et al. 2020; Suckale et al. 2016; Woitischek et al. 2020) (Fig. 3b). Gas 'hold-up' (accumulation of gas within the magma) occurs when gas supply from depth is balanced by gas loss from the system and may be implicated as a triggering mechanism for paroxysmal eruptions more generally. For example, paroxysmal eruptions are often preceded by increases in the height of the magma column which may be caused by gas retention; the resulting lava effusion from either flank (Stromboli) or summit (Fuego) vents may then trigger decompression of the shallow conduit (Calvari et al. 2011; Liu et al. 2020b; Ripepe et al. 2015). Similarly, correlations between lava lake surface elevations and gas flux at Villarrica (Johnson et al. 2018), Erta Ale (Bouche et al. 2010) and Masaya (Aiuppa et al. 2018; Williams-Jones et al. 2003), for example suggest that temporal fluctuations in deep (> 1–2 km) gas supply may be important in modulating surface activity at open-vent volcanoes and in advecting heat to maintain an open state.

Degassing throughout the magmatic system

The introduction of gas into shallow (top few km) reservoirs and conduits derived from deeper (> 2–3 km) in the system requires a mechanism of deep volatile exsolution. The principal source of that deep MVP is crystallisation and second boiling, which can generate the equivalent of several weight percentages for andesite and dacite magmas (Fig. 2b). The MVP will initially be CO_2 rich, with increasing water for higher degrees of crystallisation (Fig. 2b). Once formed, the MVP can migrate upward and out of the crystal-rich magma reservoir and rise towards the surface (Degruyter et al. 2019; Huber et al. 2010; Parmigiani et al. 2017). Given that the ratio of intrusive to extrusive magmatism is thought to be high in all tectonic settings (from an average of 3:1 to 10:1 or higher in many arc regions) (Crisp 1984; White et al. 2006) and that plutonic rocks are generally volatile-poor (Bachmann et al. 2007), it follows that the volatiles outgassed persistently by open-vent volcanoes likely have their source, at least in part, in second boiling processes in crustal reservoirs. Evidence for this deep (> 2–3 km and perhaps extending into the mid or lower crust in some cases) MVP is provided by the 'excess sulphur' emissions accompanying large explosive eruptions of arc volcanoes, which have been explained by sulphur partitioning into substantial

accumulations of an exsolved MVP in magma reservoirs (Andres et al. 1991; Rose et al. 1982; Scaillet and Pichavant 2003; Wallace and Gerlach 1994; Webster and Botcharnikov 2011; Zajacz et al. 2012). A deep-derived MVP is also implicated in gas fluxing observed in the volatile systematics of many melt inclusion suites (Blundy et al. 2010; Caricchi et al. 2018; Métrich and Wallace 2008), as well as in the diffuse degassing of CO_2 along rifts (Foley and Fischer 2017) and other volcanic centres (Werner et al. 2019). Questions remain as to the MVP source depth and mechanism(s) by which a deep-derived MVP segregates and migrates through crustal magma storage regions.

At low melt viscosities and low crystal fractions, bubbles may accumulate in foam layers at the roof zones of eruptible melt lenses (Jaupart and Vergniolle 1989; Vergniolle and Jaupart 1986) and on foam collapse, bubbly plumes may be generated (Degruyter et al. 2019; Parmigiani et al. 2016) (Fig. 3d). At intermediate crystal fractions in more evolved systems, the MVP generated through deep (> 2–3 km) crystallisation and periodic influx from mafic recharge may rise buoyantly through crystal-rich mush via viscous elongate fingering channels, which produce high permeability pathways for a deep MVP phase to percolate (Fig. 3e) (Degruyter et al. 2019; Parmigiani et al. 2016). MVP accumulation in melt-rich caps or lenses may aid eruption of crystal-poor rhyolites (Bachmann and Bergantz 2004). At high crystal fractions, the MVP may become trapped and accumulate in pore spaces between crystals; it may escape on ductile or brittle deformation (capillary fracturing) when the crystal framework is disrupted (Belien et al. 2010; Oppenheimer et al. 2015; Parmigiani et al. 2016) (Fig. 3f).

Aims of this paper

It is clear that a universal paradigm is required that applies to all open-vent volcanoes, of all magma types (high and low viscosity), and which addresses important questions such as how and where the MVP forms and its mode of its transport through the magmatic system. We review outgassing from open-vent volcanoes and lay out the characteristic and generic features common to all settings and all magma compositions. In particular, we examine how new insight into the dynamic nature of crustal magma systems, including conceptual models of volcanic-plutonic systems linked by eruptible melt lenses and unstable volatile-rich fluids (Cashman et al. 2017; Christopher et al. 2015), help us to understand persistent outgassing and gas-rich eruptions from open-vent volcanoes. More specifically, we assess the contribution of unerupted magmas and extensional tectonics to the outgassing fluxes observed at open-vent volcanoes. In considering not only the outgassing characteristics, but also the available evidence for the form and extent of the underlying magmatic system using petrology, geophysics and modelling, we outline a generic picture for understanding the volatile budget of these volcanoes.

Key observations of open-vent volcanic outgassing

Outgassing fluxes from open-vent volcanoes are decoupled from eruptions

Recent observations of volcanic outgassing from space have highlighted the number and diversity of open-vent volcanoes that emit the overwhelming bulk of volcanic gases into the atmosphere every year (Fig. 1; Table S1). Global satellite-based monitoring of volcanic gas emissions demonstrate unequivocally that > 90% of the global outgassing fluxes of sulphur dioxide are produced during 'passive degassing' from an open-vent, where no eruption is taking place (Carn et al. 2017; Fioletov et al. 2016; Werner et al. 2019). These open-vent volcanoes erupt magmas of a wide range of compositions and rheological properties (Table S1), from low viscosity basalt to highly viscous crystal-rich andesite. Moreover, as our understanding of volcanic outgassing increases, it is becoming ever clearer that 'excess' volcanic gas (over that which can be supplied by erupting magma) is the norm, rather than the exception (Andres et al. 1991; Francis et al. 1993). Here we review the gas emission systematics from a number of persistently degassing volcanoes with a wide range in magma compositions and rheological properties, eruptive style and setting.

The flux of sulphur dioxide is commonly used as a proxy for the total volatile flux from a volcano (Aiuppa et al. 2008). In most cases, SO_2 makes up 1–10 mol% of the gas phase from open-vent volcanoes, with the bulk of the gas composed of water and CO_2 in variable proportions. These two major gas species (H_2O and CO_2) are not easily measured, however, owing to their large and variable concentrations in the background atmosphere. SO_2, in contrast, has a distinct and strong absorption in the UV region (Hoff and Millan 1981) and is not present in the background atmosphere, making it ideal for monitoring volcanoes.

Etna Volcano (Italy) is an archetypal 'open-vent' volcano. It has long been observed that the persistent gas fluxes from Etna are too high to be supplied by the erupting magma (Allard 1997). SO_2 fluxes between 1975 and 1995 varied from < 1000 t/day during quiescent degassing to > 10,000 t/day during fountaining (Allard 1997). Since then, Etna has continued to outgas at prodigious rates (Andres and Kasgnoc 1998; Caltabiano et al. 1994; Salerno et al. 2009), with average SO_2 outgassing rates from 2005–2015 determined from space-based inventories showing an average rate of 2039 t/day (Carn et al. 2017). Approximately 25–30% of that SO_2 flux can be accounted for by decompression-driven

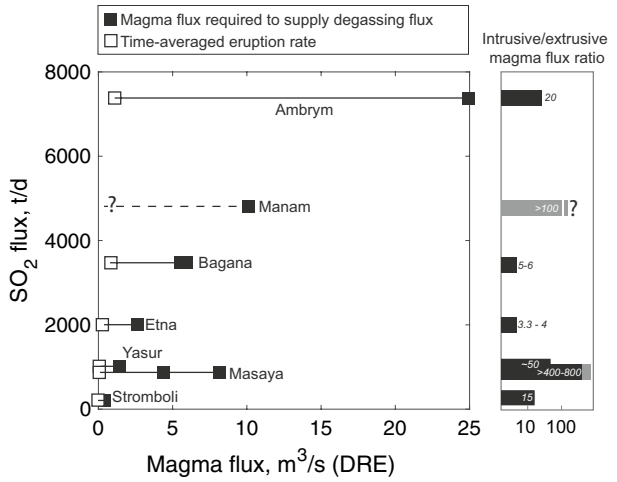

Fig. 4 A plot of mean outgassing SO_2 flux (from Carn et al. 2017) against magma flux for a range of volcanoes. The magma flux required to supply the SO_2 flux is shown as a black square and the time-averaged eruption rate is shown as an open square. Estimates of degassing and erupted magma flux are sourced from Ambrym (Allard et al. 2016); Manam (Liu et al. 2020a); Bagana (McCormick Kilbride et al. 2019; Wadge et al. 2018); Etna (Allard 1997; Allard et al. 2006); Yasur (Métrich et al. 2011); Masaya (Zurek et al. 2019) and Stromboli (Allard et al. 2008). The individual studies use a combination of melt inclusion evidence and observed gas fluxes to infer the flux of degassing magma and geological evidence to infer the magma eruption rate (please see papers for detail)

degassing of erupted magma (Fig. 4). The high rate of volatile outgassing has been attributed to continuous, convective bimodal flow, whereby alkali basalts ascend to shallow pressures, degas and then sink back down into the edifice (Allard 1997; Burton et al. 2003; Kazahaya et al. 1994), although there is little definitive geophysical or geochemical evidence to support this.

Yasur Volcano (Vanuatu) is a persistent and continuous outgasser with small-scale strombolian activity interspersed with larger paroxysms (Kremers et al. 2012; Métrich et al. 2011; Suckale et al. 2016; Woitischek et al. 2020). Anecdotal and historical evidence suggest that continuous degassing has been taking place for several centuries (Métrich et al. 2011). Frequent, strombolian eruptions eject small volumes of crystal-rich trachybasalt generated in shallow reservoirs by ~ 50% crystallisation of more primitive alkali basalts (Métrich et al. 2011). SO_2 fluxes ranged from 400–700 t/day during field campaigns in 2006, 2010 and 2018, with much of the SO_2 emitted by passive degassing between explosions (Bani and Lardy 2007; Ilanko et al. 2020; Métrich et al. 2011; Woitischek et al. 2020). Again, the gas budget cannot be accounted for by degassing of erupted magma (Fig. 4); instead, the SO_2 flux requires complete degassing of 0.04–0.05 km^3 per year of unerupted magma, which is ~ 50 times that erupted (Métrich et al. 2011; Woitischek et al. 2020). If the recent measurements are extrapolated to the past, > 4 km^3 degassed magma has accumulated beneath Yasur over the past 100 years (Métrich et al. 2011).

Manam, a basaltic stratovolcano in the Western Bismarck arc, is one of the most active volcanoes in Papua New Guinea. Continuous outgassing from two summit craters has been sustained at least over the past few decades (Carn et al. 2017; Liu et al. 2020a). Sporadic strombolian eruptions produce low-level ash plumes and are punctuated by occasional paroxysmal eruptions involving lava fountaining, lava flows, pyroclastic density currents and high ash plumes; five explosive events between August 2018 and June 2019 produced > 10-km-high eruption plumes. Manam is among the most prolific volcanic outgassers globally, with an average SO_2 flux of 1480 t/day between 2005 and 2015 (Carn et al. 2017) and a 2019 campaign measured fluxes ≤ 7660 t/day over several days (Liu et al. 2020a). Assuming an undegassed magmatic sulphur content of ~ 2000 ppm, this large SO_2 flux requires around 0.33 km^3 of magma to degas every year, which is likely to be an order of magnitude, and perhaps two, more than the erupted volume (the erupted volumes have not yet been quantified) (Fig. 4).

Some of the most prolific and/or persistent global outgassers are lava lake volcanoes (Carn et al. 2017), including Nyiragongo and Nyamuragira (Democratic Republic of Congo), Ambrym (Vanuatu), Masaya (Nicaragua), Erebus (Antarctica), Erta Ale (Ethiopia) and Kilauea Volcano (Hawaii, USA). Degassing from the surface of a lava lake takes the form of vigorous bubbling, low fountains, bubble bursting, gas pistoning and overturn and resurfacing phenomena (Allard et al. 2016; Bani et al. 2012; Bouche et al. 2010; Harris et al. 2005; Oppenheimer et al. 2009; Patrick et al. 2016; Swanson et al. 1979), with upwelling and divergence zones providing evidence for rapid lateral magma motion across the lake's surface (Harris 2008; Harris et al. 2005; Lev et al. 2019; Pering et al. 2019). These observations, as well as the high gas fluxes (a mean of 7356 t/day SO_2 from Ambrym between 2005 and 2015, with peaks reaching > 20,000 t/day SO_2) (Bani et al. 2009) and the necessity for a continuous heat source to keep the lake above its solidus temperature, have led to prevailing models of bimodal flow in the conduit to supply both sufficient volatiles and heat (Kazahaya et al. 1994; Oppenheimer et al. 2009; Oppenheimer et al. 2004; Palma et al. 2011). Although analogue experiments can reproduce bimodal flow (Palma et al. 2011; Witham and Llewellin 2006), we note that simple gas fluxing through the lava lake may supply sufficient heat and volatiles to satisfy observational requirements. For example, degassing at the surface of the Erta Ale (Ethiopia) lava lake occurs at fixed positions that are inferred to be directly above the conduit (Bouche et al. 2010). Here visual, thermal and acoustic observations suggest that spherical cap bubbles rise to burst at the surface; bubbly wakes that detach from the bubble bottom generate small fountains

and hold sufficient heat to ensure that the lava lake does not cool over time. In this scenario, a deep (> ~ 1 km) source of gas is required, with no requirement for large-scale vertical bimodal flow. Moreover, the dynamics of bubble behaviour within lava lakes may modulate degassing (Qin et al. 2018).

Intermediate composition magmas can also feed open-system vents, as illustrated by Soufrière Hills Volcano, Montserrat and Santiaguito Volcano, Guatemala. Soufriere Hills erupts high viscosity (10^9–10^{12} Pas) crystal-rich andesite (Melnik and Sparks 2002). In contrast to the mafic systems, the typical eruptive style is lava dome growth interspersed with episodes of vulcanian activity. SO_2 fluxes here have been sustained since the onset of eruptive activity in 1995 (Christopher et al. 2015; Christopher et al. 2010; Edmonds et al. 2010; Edmonds et al. 2014) and high gas emission rates have continued (to at least 2021) since the cessation of eruptive activity in 2011. SO_2 fluxes have fluctuated between < 100 and > 2500 t/day throughout the eruption (Christopher et al. 2015; Nicholson et al. 2013), with the highest SO_2 fluxes observed immediately after large dome collapses that exposed the conduit (e.g. July 1998, July 2003) (Herd et al. 2005). SO_2 fluxes were high and sustained during periods of both lava dome growth and prolonged (months-years) periods during which the eruption paused (Christopher et al. 2015; Edmonds et al. 2010). Petrological studies indicate that prior to eruption, sulphur solubility in the rhyolite melt was low (< 100 ppm) (Edmonds et al. 2001), consistent with the partitioning of sulphur into an exsolved MVP in the shallow storage region beneath the volcano (Clémente et al. 2004; Edmonds et al. 2001; Edmonds et al. 2002). The high bulk viscosity of the magma precludes convective flow as a viable mechanism to supply the outgassing fluxes; sustained degassing during eruptive pauses therefore requires both persistent permeable pathways from depth to the surface and tapping of a substantial pre-segregated reservoir of exsolved volatiles (Christopher et al. 2015).

Bagana Volcano (Papua New Guinea) has exhibited long-lived and continuous degassing, perhaps over centuries (McCormick et al. 2012; McCormick Kilbride et al. 2019; Wadge et al. 2018). Bagana's edifice is built of crystal-rich andesite lava flows and tephra (53–58 wt% SiO_2) and eruptive activity is characterised by the emplacement of steep-sided lava flows, pyroclastic density currents and ash-rich explosions (Bultitude and Cooke 1981; Wadge et al. 2018). Observations (predominantly by satellite radar) indicate that eruptive activity is strongly pulsatory, with eruptive periods separated by periods of repose, throughout which strong degassing continues (Wadge et al. 2018). SO_2 fluxes at Bagana were first measured in 1983 and reported at > 3000 t/day (McGonigle et al. 2004). A recent global inventory of volcanic SO_2 emissions measured via satellite-mounted UV sensor (ozone mapping instrument (OMI)) reported Bagana's mean SO_2 flux as 1380 t/day for the period 2005–2015 (Supplementary Material Table 1), placing it 3rd in the global ranking of sustained SO_2 fluxes (Carn et al. 2017). The highest SO_2 fluxes occur during eruptive periods (up to 10,000 t/day) but gas emissions remain high (≤ 2500 t/day) during eruptive pauses (McCormick Kilbride et al. 2019). These high gas emissions cannot be supplied by the erupted magma, which has a time-averaged eruption rate of 1 m^3/s (Wadge et al. 2018) (Fig. 4). Instead, the observed rates of degassing from 2005–2015 require around 5–6 times the observed magma flux when reasonable water and sulphur melt concentrations for arc magmas are assumed (McCormick Kilbride et al. 2019).

To summarise, although a model of conduit convection may explain persistent degassing at some volcanoes, it does not supply a universal explanation. In particular, the conduit convection model predicts that high viscosity must be compensated by a larger conduit radius in order to supply gas at a similar rate to a lower viscosity system, yet there is no observational evidence for a systematic linear relationship between magma viscosity and conduit radius. This problem is exacerbated by the lower solubility of sulphur in rhyolitic melts (Clémente et al. 2004). Additionally, a convective model requires large accumulations of degassed magma in the shallow crust, which poses a substantial space problem for long-lived open-vent systems. Water-rich magmas may completely crystallise during slow ascent, severely inhibiting return flow. A more parsimonious explanation for high gas flux across all volcano types is that gases are supplied from a mixture of shallow (conduit) and deep (> 1–2 km and perhaps as deep as the mid-crust) sources. Importantly, the flux of gases supplied from deeper magma storage regions to the shallow systems has the potential to both modulate and trigger eruptive activity and advect heat; this model also allows for degassed magma accumulations to be distributed over a substantial depth range.

Gas compositions at open-vent volcanoes are consistent with mixing between deep and shallow degassing sources

Additional information about how gases are delivered to the surface and from what depth they are sourced comes from measurements of changes in volcanic gas compositions with eruptive activity. There has been immense progress in quantifying the composition of volcanic gas emissions over the past two decades (specifically the relative abundance of H, C, S and Cl species), principally driven by instrumentation development (Aiuppa et al. 2010; Aiuppa et al. 2006; Liu et al. 2020a; Pering et al. 2020; Shinohara et al. 2008). Figure 5 shows a compilation of gas composition data from a range of volcanoes, many of which have open vents (not discriminated on the diagram). Volcanic gases are rich in

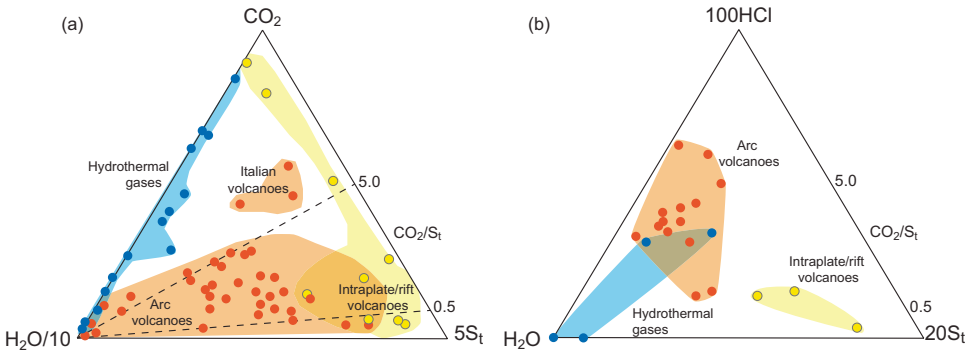

Fig. 5 A review of volcanic gas compositions. **a** H_2O–CO_2–S_t (i.e. $SO_2 + H_2S$) and **b** H_2O–HCl–S_t (i.e. $SO_2 + H_2S$) gas compositions for a range of volcanoes, made up of both direct sampling (Fischer 2008; Hammouya et al. 1998; Symonds et al. 1994) and Multigas data (Aiuppa et al. 2008; Aiuppa et al. 2015; Burton et al. 2007; Sawyer et al. 2008; Shinohara and Witter 2005). Red shaded regions = arc volcano emissions; blue = hydrothermal emissions and yellow = intraplate/rift emissions

H_2O and CO_2 and arc volcanoes are typically richer in Cl than rift or intraplate volcanoes. Although we do not consider hydrothermal systems here, we note that gases from volcanoes hosting a large hydrothermal system are typically depleted in S and HCl and rich in H_2O and CO_2. Finally, Fig. 5 shows the large variability in the molar H_2O/CO_2, C/S and S/Cl ratios measured in volcanic gases at the surface.

Before scrutinising the natural data, it is useful to construct a framework for volcanic gas compositions to understand how gas ratios may evolve during (a) decompressional degassing (with some crystallisation) and (b) isobaric equilibrium crystallisation in a magma storage region in the crust (second boiling). We use *MagmaSat* (Ghiorso and Gualda 2015b) to model the solubility of H_2O and CO_2 under different pressure, temperature and oxygen fugacity conditions (as shown in Fig. 2). Three examples are considered—Yasur, Stromboli and Soufrière Hills—using appropriate basaltic and andesitic compositions (typical erupted magma compositions for three examples are given in table S2, supplementary material). For example, to initialise a decompressional degassing model for Yasur trachybasalt (Fig. 6a), we use a water content of 1 wt% and a CO_2 content of 0.2 wt%, consistent with petrological studies of melt inclusion compositions (Métrich et al. 2011). Initial melt volatile contents are further modified by crystallisation during magma ascent, which we model using RhyoliteMelts (Ghiorso and Gualda 2015a). We model chlorine and sulphur exsolution using both a closed- and open-system partitioning model (see supplementary material for details).

We use a suite of D_{Cl} (fluid-melt partition coefficient for chlorine) values collated from the literature (Kilinc and Burnham 1972; Lesne et al. 2011; Shinohara 1994; Tattitch et al. 2021; Webster et al. 1999; Webster et al. 2017). D_{Cl} is low (< 10) for basaltic compositions and decreases as pressure decreases (Tattitch et al. 2021), although the solubility behavior of Cl is complex and varies with melt composition (Métrich and Rutherford 1992; Métrich and Rutherford 1998; Signorelli and Carroll 2002), fluid composition (Botcharnikov et al. 2004), temperature, oxygen fugacity and pressure (Botcharnikov et al. 2004; Webster et al. 2009); a review is presented in the supplementary material. Some studies have postulated an inverse relationship between D_{Cl} and pressure, i.e. that D_{Cl} decreases with increased pressure (Alletti et al. 2009; Shinohara 2009); this is explained by the large and negative pressure dependence of NaCl partitioning into a melt and the HCl–NaCl exchange reaction between a silicate melt and an aqueous fluid, which favours HCl in aqueous fluids at lower pressures (Shinohara 2009). These pressure dependencies cause chlorine to appear as HCl in low pressure (~ 0.1 MPa) volcanic gases and NaCl in high pressure (~ 50 MPa) fluids. More work is required, however, to fully understand the implications of Cl speciation on fluid-melt partitioning (Shinohara 2009).

We use D_S (fluid-melt partition coefficient for sulphur) values derived from experiments at high pressure and temperature using natural basalt samples from Masaya and Stromboli (Lesne et al. 2011), which range from 1 to 5 at pressures > 200 MPa and > 100 for pressures < 50 MPa (Fig. 6a). Lesne et al. (2011) used synthetic samples based on natural Stromboli melts with an initial volatile inventory representing the most volatile-rich melt inclusions from each volcano. For more evolved compositions, we use partition coefficients derived from experiments (Botcharnikov et al. 2004; Botcharnikov et al. 2015; Webster and Botcharnikov 2011). These indicate that the fluid-melt partition coefficient for sulphur increases with melt differentiation, reaching values of > 500 for rhyolitic melts, and likely increases as the melt water content decreases during decompression (Moune et al. 2009). Model results for Yasur, Stromboli and Soufriere Hills are shown in tables S3, S4, S5.

A second set of models (a Yasur example is shown in Fig. 6b) simulates isobaric, closed-system degassing during

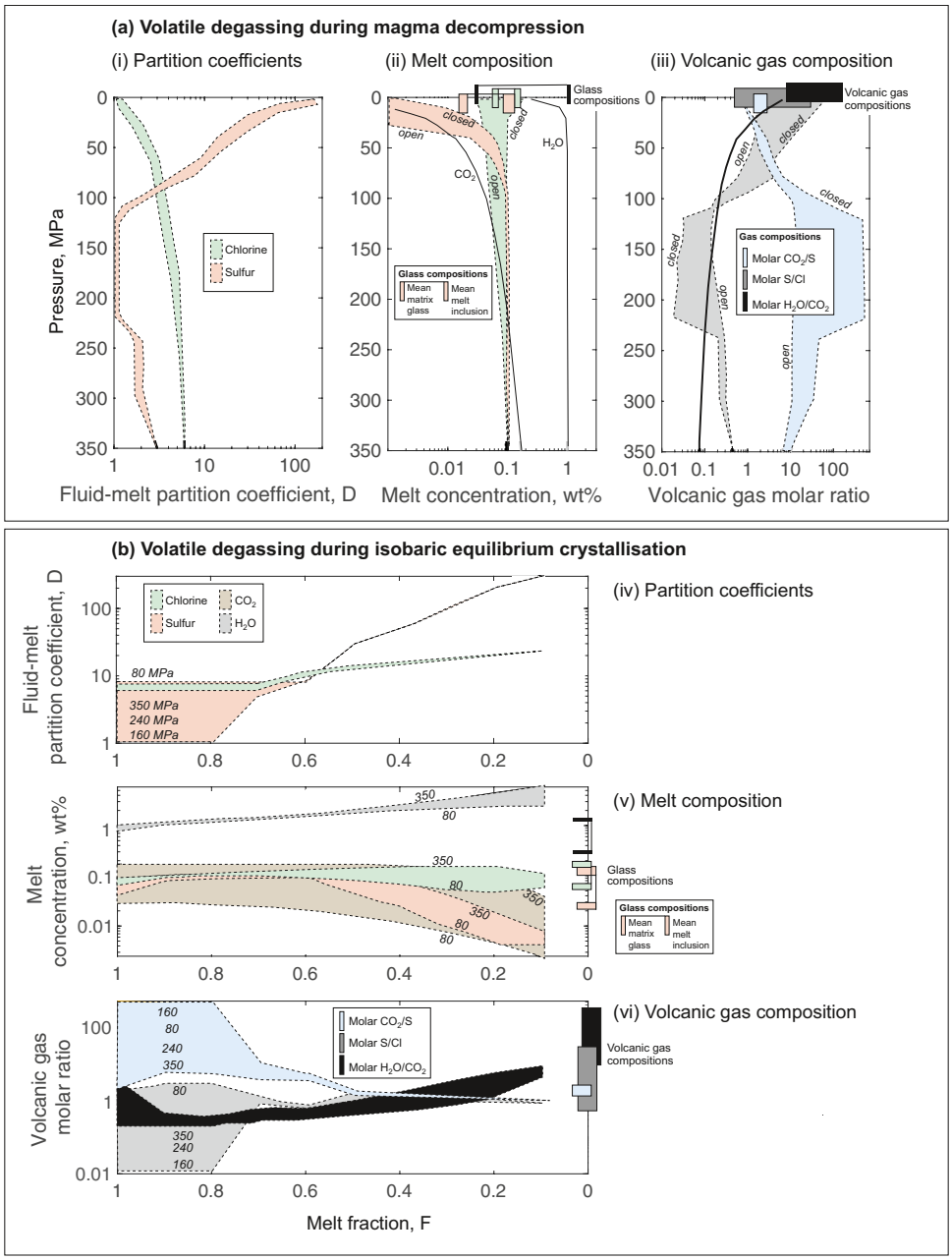

Fig. 6 Models reconstructing the degassing of volatiles during decompression degassing and during isobaric crystallisation of alkali basalt melts at Yasur Volcano, Vanuatu. **a** Decompression of a trachybasalt from Yasur is accompanied by the exsolution of water and CO_2 (using Magmasat (Ghiorso and Gualda 2015a) from initial values of 1 wt% and 0.2 wt% respectively, based on melt inclusion and volcanic gas studies (Métrich et al. 2011; Woitischek et al. 2020). Fluid melt partition coefficients for Cl and S are shown in (i), melt volatile concentrations in (ii) and exsolved volatile phase composition in (iii). Open- and closed-system degassing models are considered, where open-system degassing incorporates integration of the gas phase of the magma column at each pressure step. **b** Isobaric crystallisation leads to second boiling through enrichment of the melt in volatiles. Shown here are fluid-melt partition coefficients for Cl and S (i), melt volatile concentrations (ii) and the composition of the exsolved volatile phase (iii) for crystallisation models (from a melt fraction, F, of 1 to a melt fraction of 0.1) at pressures of 80, 160, 240 and 350 MPa. The pressures of crystallisation are marked to show how the range in compositions links to pressure. Details of the models are given in supplementary material. Observed glass compositions (Métrich et al. 2011) and volcanic gas compositions (Oppenheimer et al. 2006; Woitischek et al. 2020) are marked on **a** and **b**

crystallisation for four example pressures between 80 and 350 MPa, thus representing magma stored in the crust that undergoes second boiling (details of the model are given in the supplementary material; results are shown in tables S6, S7 and S8). The melt concentrations of H_2O, CO_2, Cl and S, together with the molar fractions of each in the exsolved

volatile phase, are shown in Fig. 6(v) and 6(vi) as a function of melt fraction. The observed compositions of the volcanic gas at Yasur are shown in Fig. 6(iii) and 6(vi) for comparison (Métrich et al. 2011; Woitischek et al. 2020), and glass compositions are shown in Fig. 6(ii) and 6(v) (Métrich et al. 2011). It is important to note that the models shown here incorporate a significant amount of uncertainty; we use them to define the general trends expected for magma degassing under a range of conditions.

The degassing behaviour of Yasur magmas (Fig. 6) shows an exsolved volatile phase that evolves from carbon- and chlorine-rich compositions at high pressures, to sulphur- and water-rich compositions at low pressures, consistent with our understanding of the effect of pressure on solubility and partitioning (Fig. 6a, b; table S3). Exsolved volatile phase C/S ratios attain a maximum (of > 300 for closed-system degassing and ~ 10 for open-system degassing) at pressures of 100–230 MPa (Fig. 6(iii)). Sulphur is preferentially exsolved over Cl at low pressures, leading to a sharp increase in exsolved volatile phase S/Cl ratios and a sharp drop in the S/Cl ratios of melts at P < ~ 100 MPa (Fig. 6(ii, iii)). The ranges in X^{S}_{melt} and X^{Cl}_{melt} thus derived match well with ranges of these elements preserved in melt inclusions and matrix glasses from Yasur (Fig. 6(ii)) (Métrich et al. 2011). More generally, model predictions are consistent with published measurements of volatile concentrations in melt inclusion and groundmass glasses at Stromboli, Yasur and Etna (Métrich et al. 2011; Métrich et al. 2010; Métrich and Wallace 2008; Spilliaert et al. 2006) and observed in the closed-system experiments of Lesne et al. (2011).

The exsolved volatile phase is expected to have a molar C/S of 10–100 at pressures > 100 MPa, decreasing from ~ 10 at 80 MPa to ~ 1 at the surface. Volcanic gases at Yasur have a molar C/S of ~ 2–3 (Métrich et al. 2011; Woitischek et al. 2020), consistent with gases being sourced from integrated, open-system degassing of the entire magma column to a pressure of 80 MPa (< 3 km depth). Open-system degassing is expected; the basalt has a low viscosity (< 1000 Pa s (Giordano et al. 2008)) and bursting of large bubbles at the surface is the dominant style of activity (Kremers et al. 2012; Woitischek et al. 2020). Volcanic gases have a molar S/Cl ratio of ~ 0.5 to 30 (Woitischek et al. 2020; Métrich et al. 2011; Oppenheimer et al. 2006); this is again consistent with open-system degassing of the entire magma column to a pressure of 80 MPa (Fig. 6(iii)).

Importantly, observations of volcanic gases, whilst consistent with models of decompressional degassing, are also consistent with a fraction of the gases being derived from a deep (> 2–3 km) exsolved volatile phase generated during prolonged crystallisation (Fig. 6b). In this scenario, as magma evolves from basalt to trachybasalt (at 80 MPa, after about 50% crystallisation), it generates ~ 0.6 wt% exsolved fluids. The exsolved volatile phase is carbon and chlorine-rich at melt fractions ≥ ~ 0.7 (Fig. 6(vi)), then crystallise at molar C/S ratios of ~ 1.5–2.5 and molar S/Cl ratios of 1–2. These values are consistent with volcanic gas compositions observed at the surface (Fig. 7a), which raises the possibility that some, and perhaps a large fraction, of the gases fluxing through the conduit and into the atmosphere may be derived from the fluids produced during equilibrium crystallisation of basalts at depths of ~ 3 km or deeper. Indeed, Métrich et al. (2011) concluded from melt inclusion geochemistry that primitive basalts pond at ~ 3-km depth where they fractionate during ~ 50–60% crystallisation to form trachybasalts with 56–60 wt% SiO_2. 50% equilibrium crystallisation would produce ~ 1000 ppm exsolved S, ~ 1000 ppm exsolved Cl and 0.3 to 0.6 wt% H_2O (Table S2; Supplementary Material); this would require the intrusion of

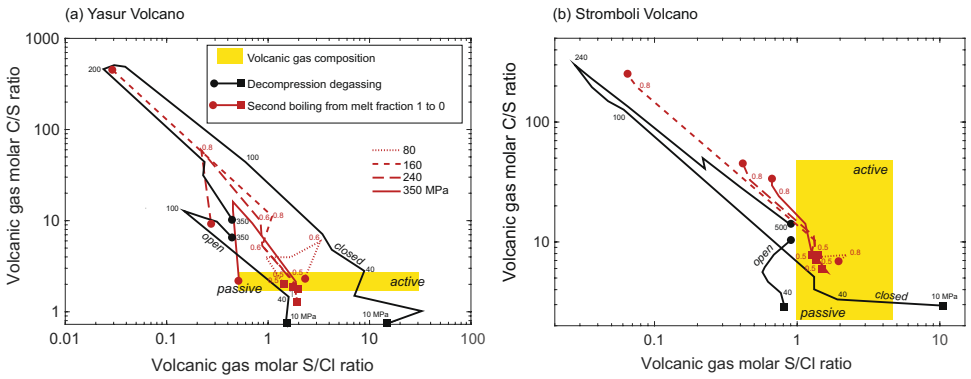

Fig. 7 Composition of the exsolved volatile phase with pressure and melt fraction for **a** Yasur, Vanuatu, and **b** Stromboli, Italy. Shown in solid black lines in both **a** and **b** are the decompressional degassing models for open- and closed-system degassing, marked with some of the pressure steps, in MPa. Dashed and red lines (see legend) are the isobaric second boiling models to describe the exsolved volatile phase produced during equilibrium crystallisation and degassing at various pressures, marked in red with the melt fraction remaining (1 to 0, where 1 is the case where there is no crystallisation, 0 denotes fully crystallised). A yellow box marks the compositions of volcanic gases observed at the surface (Aiuppa et al. 2010; Allard 2010; Oppenheimer et al. 2006; Woitischek et al. 2020)

0.04–0.09 km^3 magma/year, similar to the volume required for the postulated vertical large-scale convection to shallow depths necessary to supply outgassed SO_2 and HCl. Furthermore, the latent heat generated by extensive shallow magma crystallisation may be sufficient to thermally buffer the magma reservoir and to maintain a hot conduit (Métrich et al. 2011). Ascent of a deep-derived exsolved volatile phase, possibly with subsidiary melt, could advect heat to the conduit, allowing it to remain at a constant temperature over decadal timescales.

Importantly, fluids generated by second boiling would be relatively water-poor owing to the relatively low water content of Yasur basalts and the high solubility of water in silicate melts. The high water contents of Yasur volcanic gases (Métrich et al. 2011; Woitischek et al. 2020) would thus seem to be good evidence for some decompressional degassing and magma convection. The water content of the volcanic gases is, however, an order of magnitude higher than expected from decompressional degassing alone, which may suggest a contribution from meteoric waters. In summary, it is likely that the volcanic gases emitted to the atmosphere record mixing between exsolved volatiles generated by deep (> 2–3 km) isobaric second boiling and by decompression degassing accompanying convection, with the possible addition of shallow meteoric water, although this is not well constrained (Fig. 7a).

Gas data for Stromboli volcano (Fig. 7b) illustrate the wide range of gas compositions observed during eruptive activity (Aiuppa et al. 2010; Allard 2010; Burton et al. 2007; Tamburello et al. 2012). Stromboli's volcanic gases are dominated by H_2O (48 to 98 mol%, mean 80 mol%) and also contain CO_2 (2–50 mol%, mean 17 mol%) and SO_2 (0.2 to 14 mol%, mean 3 mol%). During paroxysms and strombolian explosions, the carbon content of the emitted gases extends to 50 mol% CO_2 with a molar C/S of > 10 and up to 47, a low molar H_2O/CO_2 (typically 1–3) and high S/Cl ratios (mean 4.7 ± 0.08). Between explosions, the gas molar C/S is < 15, H_2O/CO_2 is 1.5 to 6.5 and S/Cl is 1–1.5. Stromboli is fed by magmas with a much higher volatile content than at Yasur, as evidenced by studies of melt inclusions (Métrich et al. 2010). As an approximation of the Stromboli system, we use a starting basalt composition (Supplementary Table S1) with 3 wt% H_2O, 2 wt% CO_2, 0.2 wt% Cl and 0.25 wt% S (Métrich et al. 2010) for the modelling (details given in supplementary material).

As for Yasur, and consistent with previous studies (Aiuppa et al. 2010; Allard 2010; Métrich et al. 2010), we find that decompressional degassing of the exsolved volatile phase for Stromboli compositions causes the C/S ratio to decrease from > 100 at pressures between 240 and 100 MPa to ~ 1–2 at the surface (Fig. 7b; table S4). Also, similar to Yasur, the volcanic gas molar S/Cl ratio increases with decreasing pressure from < 0.1 at depth to 1–10 at the surface, governed by the relative partitioning behaviour of Cl and S with pressure (Lesne et al. 2011; Tattitch et al. 2021). The fluids generated during isobaric crystallisation (second boiling), in contrast, initially have low C/S and S/Cl but converge on C/S ~ 5–8 and S/Cl ~ 1–2 after 50% crystallisation.

The high molar CO_2 content of the gases during strombolian explosions and paroxysms suggest triggering by a deep-derived gas phase (Aiuppa et al. 2010; Allard 2010; Burton et al. 2007; Métrich et al. 2010), with the gases emitted during quiescent degassing fed by more shallowly-equilibrated gases. However, a comparison of gas compositions to a decompressional degassing model (Fig. 7b) shows that the SO_2/HCl systematics (Burton et al. 2007) are not obviously consistent with such an interpretation. Indeed, decompressional degassing models predict 'deeper'-equilibrated gases to have a lower S/Cl than shallow-equilibrated gases; this trend reflects the decrease in the fluid-melt partition coefficient for Cl with decreasing pressure, in tandem with a dramatic increase in the fluid-melt partition coefficient for sulphur (Lesne et al. 2011). As noted above, we have only a limited understanding of the chlorine systematics in volcanic gases. However, a likely explanation is that degassing during paroxysms is more 'closed' than during persistent degassing, consistent with the higher observed molar S/Cl as well as the high molar C/S. The observed S/Cl ratio of ~ 2 of the quiescent plume at Stromboli (Burton et al. 2007), which accounts for the bulk of the outgassing flux (Allard et al. 2008), is equally consistent with an exsolved volatile phase being generated by decompression degassing or by second boiling processes at depth or a mixture of both sources (Fig. 7b).

Petrological studies provide additional constraints on the Stromboli magmatic system. Stromboli is fed by primitive, volatile-rich high K_2O (HK) basalts with 49–51 wt% SiO_2 and CaO/Al_2O_3 > 0.6 (Métrich et al. 2010) stored at depths of 7–10-km beneath the summit (Bertagnini et al. 2003; Métrich et al. 2010). Large paroxysms erupt this low-density CO_2-rich HK basalt as 'golden pumice' (Pichavant et al. 2009; Rosi et al. 2000), with little evidence for mixing with shallow-stored magma, consistent with rapid and primarily closed-system decompression (Métrich et al. 2021; Pichavant et al. 2009). Eponymous strombolian activity, in contrast, ejects crystal-rich, degassed shoshonitic basalt (51–54 wt% SiO_2) stored at 2–4-km beneath the summit and produced by 20–30% fractional crystallisation of HK basalts at depth (Landi et al. 2004; Métrich et al. 2010; Métrich et al. 2001; Métrich et al. 2005; Vergniolle and Métrich 2021). Deep and shallow magmas mix only during smaller paroxysms (LaFelice and Landi 2011a). CO_2-rich fluids derived from ponding and crystallising basalts at depth, in contrast, flux through the shallow system, dehydrating the overlying magma and promoting extensive crystallisation within the

shallow conduit (Landi et al. 2004; Métrich et al. 2001). Resulting crystal networks may trap rising fluids to form gas pockets; the release of these accumulated gases when they overcome the forces holding the crystals together (the effective yield strength) may explain the 'normal' strombolian activity (Barth et al. 2019; Belien et al. 2010; Oppenheimer et al. 2015; Suckale et al. 2016; Woitischek et al. 2020) that produces highly degassed, crystalline and high viscosity bombs, remnants of the degassed 'plug' (Caracciolo et al. 2021; Gurioli et al. 2014; Lautze and Houghton 2007). Triggers for paroxysmal activity, in contrast, are debated. One suggestion is that they may be triggered by rapid (days) ascent of HK magma (La Felice and Landi 2011; Métrich et al. 2010; Métrich et al. 2021) caused by increases in overpressure in the deep storage area or by the greater buoyancy of gas-rich basaltic magma (Allard 2010; Métrich et al. 2005; Métrich et al. 2021). A 'top-down' trigger has been suggested for paroxysms preceded by high gas hold-up and lava effusion, which promote decompression of the shallow conduit (Calvari et al. 2011; Ripepe et al. 2015). These contrasting scenarios raise interesting questions about the role of deep volatiles in modulating eruptive activity.

Volcanic gas compositions measured at Mount Etna (Italy) reveal that paroxysmal phases of ash emission and lava fountaining during 2001 (Aiuppa et al. 2002) and mid- and late November 2002 (Aiuppa et al. 2004) were accompanied by volcanic gases with low molar S/Cl ratios (< 1) and high SO_2 fluxes (15,000 t/day). Conversely, a trend of increasing S/Cl ratios and decreasing SO_2 flux accompanied the transition of volcanic activity towards mild strombolian activity and finally passive degassing with minor effusive activity. A sulphur and halogen degassing model developed to explain these trends (Aiuppa 2009) suggest that the S/Cl ratio in the gas phase increases by decompression degassing as magma nears the surface because of the increasing preference of Cl for the melt and of S for the gas (see Fig. 7b), as observed in geochemical studies (Spilliaert et al. 2006). The Cl-rich gas emitted during the paroxysms may therefore represent a deeper exsolved volatile phase, perhaps generated through second boiling processes at depth. Such a fluid phase would fuel the development of deep, volatile-rich melts co-existing with the Cl-rich exsolved volatile phase implicated in driving paroxysms at Etna. Evidence of high S/Cl ratios in volcanic gases during fountaining (Allard et al. 2005), in contrast, may record a large shallow influx of undegassed magma accompanied by relatively shallow degassing at low pressures.

Now that gas geochemical monitoring is commonplace, and often automated, trends prior to explosive eruptions at open-vent volcanoes are increasingly well characterised. Pulses of CO_2 are often observed prior to paroxysms and other forms of an explosive eruption, manifest as increases in the C/S ratio days to weeks prior to eruption (Aiuppa et al. 2017; Aiuppa et al. 2007; de Moor et al. 2017). At Villarrica volcano, Chile, for example, an increase in volcanic gas C/S after January 2015 preceded the 3 March 2015 paroxysm (Aiuppa et al. 2017). The same pre-eruptive period saw an increase of > 50 m in the height of the persistent lava lake (from 27 February; Johnson et al. 2018), suggesting increased gas hold-up. Similar signals preceded explosive activity at Turrialba Volcano, Costa Rica, in 2014 and 2015, where pulses of deeply derived CO_2-rich gas ($C/S_{total} > 4.5$) have been observed up to 2 weeks before eruptions (de Moor et al. 2016). These signals of 'deep-derived' exsolved volatiles, arriving at the surface in the absence of (or preceding) magma, provide further evidence of a significant, exsolved and segregated exsolved volatile phase at a depth that is capable of fluxing up through the shallow plumbing system prior to and during explosive eruptions, including paroxysms, supported by studies of gas fluxes and scoria textures, which illustrate degassing-driven mingling between deeper hotter melt and degassed, more crystallined magma derived from the upper parts of the conduit (Gurioli et al. 2008).

At intermediate open-vent volcanic systems, evolved melts with high fractions of exsolved volatiles may dominate the magma reservoir and the contribution of second boiling to the exsolved volatile phase may be far more significant. Although few long time series of volcanic gas compositions exist for these systems, one exception is Asama Volcano in central Japan, a persistently degassing volcano that erupts every few years (Shinohara et al. 2015). Here, periods of high gas flux coincide with periods of eruptions and elevated seismic activity. Low SO_2 emission rates characterise periods of low eruptive activity. SO_2/HCl ratios in the gas are high during eruptive periods and lower during eruptive pauses, a pattern consistent with eruptive periods dominated by decompressional degassing (Shinohara et al. 2015). There is no clear variation in C/S between active and inactive periods (Shinohara et al. 2015). In contrast, Soufrière Hills Volcano, which erupted crystal-rich andesite episodically between 1995 and 2011, showed a clear pattern of molar S/Cl > 1 during eruptive pauses and S/Cl < 1 during eruptive episodes dominated by lava dome building that remained consistent over many years of observation (Christopher et al. 2010; Edmonds et al. 2001). These gas characteristics can be explained by cessation of gaseous HCl flux during eruptive pauses whilst a near constant (or slowly declining) SO_2 flux is sustained (Christopher et al. 2010). The data are insufficient to assess whether systematic temporal variations in molar C/S exist.

Volcanic gas compositions arising from models of decompressional degassing versus isobaric second boiling are compared with observations in Fig. 8. The Soufrière Hills andesite is crystal rich with a rhyolitic carrier liquid; fluid-melt partition coefficients for chlorine and sulphur are estimated to be ~ 20–30 and ~ 200–500, respectively,

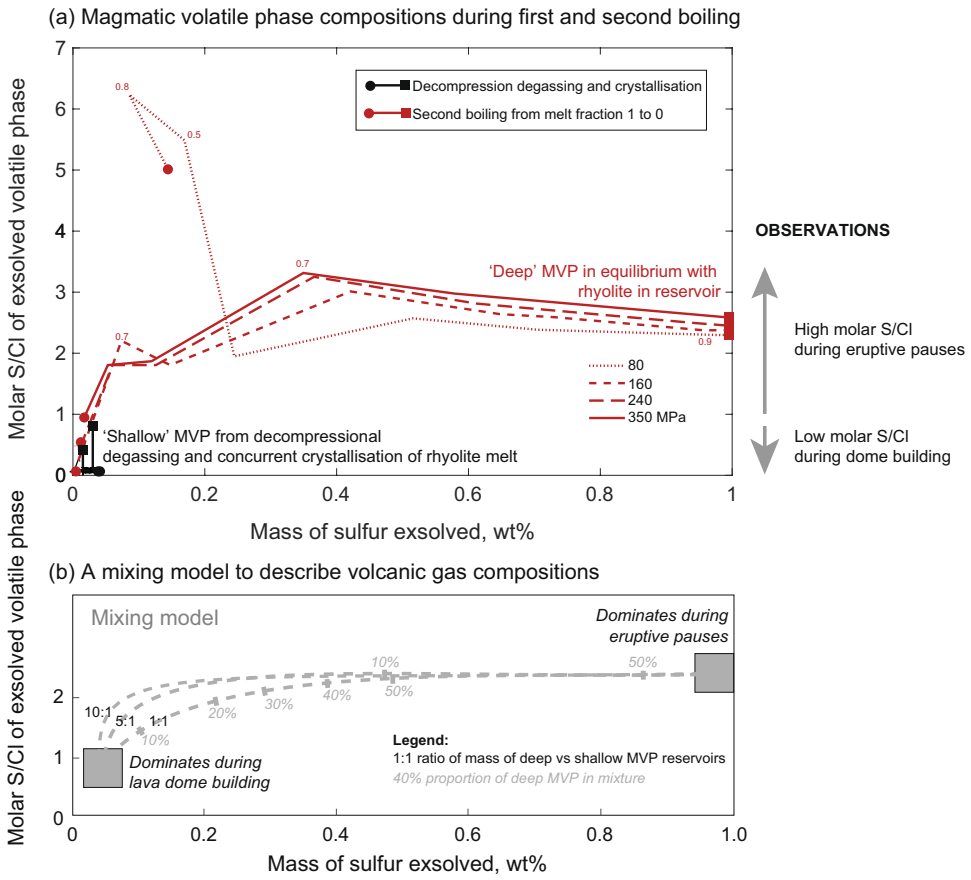

Fig. 8 Mixing between a deep-derived MVP, generated through extensive second boiling, and an MVP derived from decompressional degassing may explain the gas systematics at Soufrière Hills Volcano, where high SO_2 fluxes and low S/Cl are observed during dome building and high SO_2 fluxes and high S/Cl during eruptive pauses. **a** The molar S/Cl of the MVP varies with S outgassed (in wt% of the melt + exsolved volatile phase) for isobaric degassing during second boiling and for decompressional degassing of S-poor rhyolite. Melt fraction remaining, F, is marked onto the trajectories for isobaric second boiling. Note the composition of the 'deep' MVP in equilibrium with rhyolite will differ if different bulk magma compositions of sulphur and chlorine are used, but the relative trends shown in the figure will remain the same. **b** The volcanic gas compositions at the surface may be explained well by a mixing model whereby a deep MVP generated through second boiling mixes with an MVP generated during decompressional degassing and crystallisation of sulphur-poor crystal-rich andesite (with a rhyolitic melt phase). Depending on the relative sizes of the two MVP reservoirs, the effect of mixing on the volcanic gas composition changes. For equal-sized reservoirs in terms of the mass of the MVP phase per unit of magma, a scenario might be envisaged whereby during dome building the shallow MVP dominates, generating Cl-rich gases, and during eruptive pauses (open-vent degassing), the deep MVP dominates, generating high S/Cl gases and a high SO_2 flux

at the pressures of storage prior to eruption; with decreasing pressure, D_{Cl} decreases to ~ 1 and D_s increases to > 1000 (Tattitch et al. 2021; Webster and Botcharnikov 2011) (Tables S5, S8). Bulk chlorine and sulphur contents are poorly constrained; we use 0.15 wt% for Cl (informed by melt inclusion studies (Edmonds et al. 2001) and 0.3 wt% S for initializing the isobaric degassing models at F = 1. In general, the deep MVP generated by second boiling has an initially high molar C/S ratio, which then decreases and converges on composition of ~ 1–2 after ~ 60% crystallisation at a range of pressures (Table S8) and an initially low molar S/Cl ratio that increases and converges on values between 2 and 3 (Fig. 8a). These values yield Cl and S melt concentrations of 700–1000 ppm Cl and 50–100 ppm S after 90% crystallisation, consistent with melt inclusion studies of SHV rhyolitic melt inclusions (Edmonds et al. 2001) (Table S3, supplementary material). After the 90% crystallisation required to generate rhyolite melt, there is 4–7 wt% exsolved water-rich MVP (supplementary material table S8) with a molar C/S of ~ 1. Rhyolitic melts beneath Soufrière Hills Volcano are therefore likely to have significant fractions of MVP that must be migrating to the surface, even during eruptive pauses, to supply the outgassing flux (Christopher et al. 2015).

Rhyolitic melt starting with 8 wt% H_2O, 1 wt% CO_2, 0.1 wt% Cl and 0.01 wt% S (consistent with the melt concentrations measured in melt inclusions, table S3) subjected to slow degassing-induced crystallisation yields a Cl-rich

volcanic gas (Fig. 8a; table S5), consistent with the S-poor melt. Variable mixing between the deep (> 2–3 km) MVP generated during second boiling and a decompression-derived MVP during eruptions could thus yield a volcanic gas with a low S/Cl ratio during eruptive periods (contributions from both deep- and decompression-derived MVP) and a high SO_2 flux with a high S/Cl ratio during eruptive pauses (contributions dominated by the deep MVP generated through second boiling), which is precisely what we observe (Christopher et al. 2010; Fig. 8b). This example clearly demonstrates the importance of a segregated deep MVP in sustaining outgassing at more evolved open-vent volcanoes; this mechanism may be generic to other, similar volcanic systems globally (e.g. Tungurahua and Reventador, Ecuador; Bagana volcano, Papua New Guinea).

Geophysical evidence for the decoupled flow of an exsolved magmatic volatile phase in the crust

Seismicity related to shallow degassing and eruption

Low-frequency (LF, or long period, LP) earthquakes are a common feature of active volcanoes (McNutt and Roman 2015). When LP earthquakes are closely spaced in time, the signals may merge to form a continuous tremor signal. LP earthquakes (and tremor) are thought to be caused by fluid pressurisation, including the resonant response of fluids in conduits or dykes (Chouet 1996; Neuberg et al. 2000). Very-long-period (VLP) and ultra-long-period (ULP) events detected using broadband seismometers originate at shallow depths (≤ 1.5 km) and are associated with eruptions or vigorous fumarolic activity (McNutt and Roman 2015; Sanderson et al. 2010). Although the specific interpretations of VLP and ULP events vary, there is general agreement that they provide evidence of short-term deformation accompanying eruptive activity (Chouet et al. 1999; James et al. 2006; Oppenheimer et al. 2020; Ripepe et al. 2015; Suckale et al. 2016). Recent studies highlight links between seismic signals and degassing flux at many open-system volcanoes (Zuccarello et al. 2013). A direct link between VLP signals and strombolian activity was first identified at Stromboli volcano: very-long-period (VLP) signals sourced from a few hundred metres depth in the conduit were thought to originate from the rise and bursting of large slugs of gas within the conduit (Chouet et al. 1999). More recent data clearly show a VLP signal preceding each event together with synchronous thermal and SO_2 flux signals accompanying each explosion (Gurioli et al. 2014; Tamburello et al. 2012). Although the form of gas transport up the conduit linked to these seismic (and infrasound) signals has long been interpreted as a rising gas slug (Blackburn et al. 1976; Jaupart and Vergniolle 1988; Ripepe et al. 2001), an alternative model calls for gas accumulation in, and release from, a crystal-rich, shallow plug (Del Bello et al. 2015; Gurioli et al. 2014; Oppenheimer et al. 2015; Suckale et al. 2016). Correlations between VLP events and degassing have also been observed at Etna (Zuccarello et al. 2013), Merapi (Hidayat et al. 2002), Asama (Kazahaya et al. 2011) and Erebus (Aster et al. 2008). Similarly, episodic explosive activity modulated by accumulation and release of a gas phase beneath a rigid or semi-rigid plugs may explain shallow (~ 300 m) VLP signals at Fuego (Waite et al. 2013) and inflation-deflation cycles and periodic explosions at Santiaguito (Bluth and Rose 2004; Johnson et al. 2014).

Seismicity and strain signals related to the migration of volatiles at depth

Deeper geophysical signals related to the movement or pressurisation by an MVP are limited. MVP-related seismic signals in the upper crust have been observed at Popocatepetl volcano, where VLP signals accompany volcanic degassing bursts at a depth of ~ 1.5 km. One interpretation is that these signals record the opening of an escape pathway for an exsolved volatile phase that accumulated because of second boiling in a shallow sill (Chouet et al. 2005). Sharper pressure transients associated with expanding gas pockets may generate VLP signals to depths of ≤ 3 km (Arciniega-Ceballos et al. 2008). Another example of the upper crustal movement of MVP comes from Soufrière Hills, where strain signals observed during vulcanian explosions and gas emission events record inflation of a shallow conduit and near-simultaneous contraction of deeper magma reservoirs (> 5-km depth) (Hautmann et al. 2014). This strain pattern has been interpreted as rapid upward migration of a buoyant MVP, initiated by a sudden destabilisation of large pockets of already segregated fluid in the magma reservoirs (Christopher et al. 2015; Hautmann et al. 2014; Linde et al. 2010).

Deep long-period earthquakes (DLPs) associated with volcanoes have been observed in the mid-lower crust or mantle (Aso and Tsai 2014; Melnik et al. 2020; Wech et al. 2020). Although their origin is enigmatic, some studies have linked DLPs to an exsolved MVP. A striking example is Mauna Kea, Hawai'i, where more than a million DLPs have been recorded in the past 19 years (Wech et al. 2020). These events are not linked to eruptions but have been ascribed to the second boiling of deep (near-Moho) magma intrusions. Other interpretations of DLPs include thermal stresses set up by cooling magmas (Aso and Tsai 2014) and rapid changes of magmatic pressure in the lower crust caused by rapid nucleation and growth of gas bubbles in response to the slow upwelling of volatile-saturated magma (Melnik et al. 2020). The latter explanation for the Klyuchevskoy volcanic group relates to primary melts that may contain ≤ 4 wt% H_2O and 0.6 wt% CO_2, which would cause volatile saturation at 800 MPa (~ 30 km). Alternatively, these DLPs may record the

pressurisation of a deep reservoir and the consequent transfer of the magma towards the surface. The relatively fast upward migration of long-period activity at Klyuchevskoy (months) suggests that a hydraulic connection is maintained between deep and shallow magmatic reservoirs (Shapiro et al. 2017) and the upward transport includes a large fluid component (Koulakov et al. 2013).

Seismic tomography within the crust beneath volcanoes yields a picture of how melt versus MVP-rich areas may be distributed (Kuznetsov et al. 2017; Londoño and Kumagai 2018; Vargas et al. 2017). A porous medium saturated with gas has a low compression modulus that yields low-velocity P-waves but no decrease in S-wave velocity (a low Vp/Vs ratio). High P-wave velocities and low S-wave velocity (high Vp/Vs ratios) may, in contrast, indicate the presence of melts, i.e. an active magma reservoir (Kuznetsov et al. 2017). In this way, repeat tomographic studies can monitor temporal changes in the structure of magmatic systems. At Nevado del Ruiz, Colombia, for example the distribution of low and high Vp/Vs regions changes on yearly timescales (Londoño and Kumagai 2018; Vargas et al. 2017). Nevado del Ruiz is an open-vent volcano with considerable fluxes of SO_2 emitted continuously (Lages et al. 2018). Here a high Vp/Vs anomaly 2-4 km prior to 2010 is interpreted as a volatile-rich melt reservoir, the lower boundary of which moved upward in 2011–2012 and was replaced by a region of low Vp/Vs, interpreted as a gas-rich region undergoing second boiling; this was associated with intense, persistent outgassing at the surface (Vargas et al. 2017). Tomographic studies of Mt. Spurr, an intermittently open-vent volcano, show finger-shaped seismic anomalies with a high Vp/Vs ratio beneath the location of intensive fumarolic activity in 2004–2005 that are interpreted to represent separate conduits of magma and volatiles (Koulakov et al. 2018). A shallow (0–2 km) region of low Vp/Vs directly above is interpreted as a large-scale degassing event, whereby gases were segregated and migrated up to the surface (Koulakov et al. 2018). Although limited, these studies illustrate the potential for future monitoring of volatile and melt distributions beneath open volcanic systems.

Open-vent persistent volcanic outgassing is promoted in complex, extensional tectonic regions

Open-vent volcanoes that generate high outgassing fluxes (Fig. 1) are often located in regions of complex tectonics and local extension. The correspondence between the locations of open-vent volcanoes and major crustal extensional structures highlights the role of tectonics in promoting magma intrusion, MVP segregation and MVP migration to the surface. Although the processes that modulate MVP behaviour are not well known, the association of persistent degassers with extensional regions suggests that (a) extension leads to high intrusive/extrusive magma ratios and therefore provides large upward fluxes of exsolved volatiles through second boiling; (b) extension may promote the gravitational segregation of low-density MVP phases in shallow reservoirs, allowing their migration and outgassing and/or (c) faults and shear zones in extensional regions may become permeable pathways for deep fluids (Fig. 9).

Many persistently degassing open-vent volcanoes—Popocatepetl (Mexico), Fuego and Pacaya (Guatemala), Turrialba and Poas (Costa Rica) and Telica and Masaya (Nicaragua)—are located within grabens along the Central American Volcanic Arc (CAVA) and Trans-Mexican Volcanic Belt (TMVB). For example, the open-vent volcano Masaya lies within a large arc-parallel basin—the

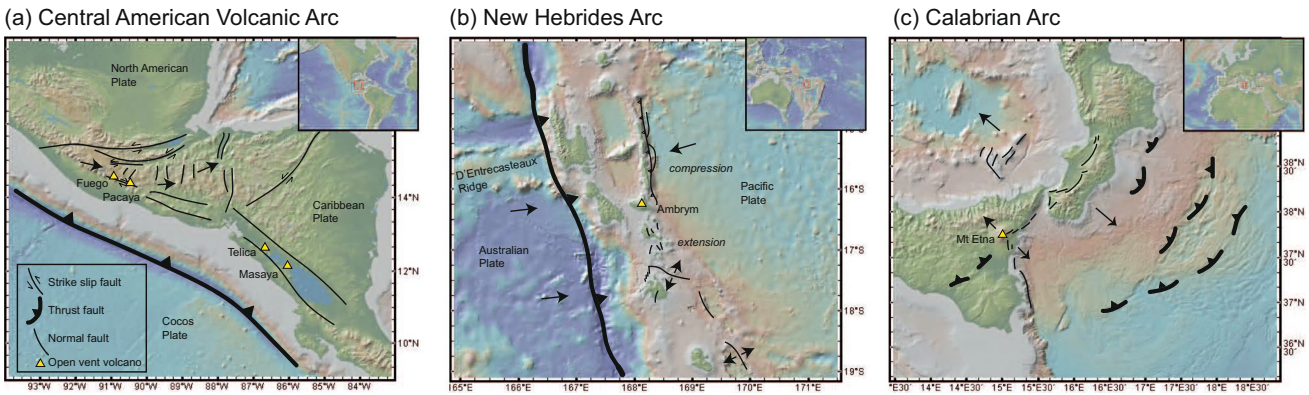

Fig. 9 Open-vent volcanoes are often in complex, extensional tectonic settings. **a** Masaya, Telica, Fuego and Pacaya, in the Central American Volcanic Arc, are closely located in regions of local crustal extension, associated with the Nicaraguan Depression (Masaya, Telica) and the rotational block tectonics of Guatemala (Fuego, Pacaya). **b** Ambrym is located at the boundary between a compressional and extensional regime in the Hebrides Arc. **c** Mount Etna, Italy, is located in an extension region stretching from Eastern Sicily to the south of Italy (see text for detail). Maps were generated using GeoMapApp

Nicaraguan graben—that contains Lake Nicaragua and Lake Managua (Morgan et al. 2008) (Fig. 1; 9a). Masaya exhibits cycles of intense outgassing that coincide with lava lake activity (Delmelle et al. 1999; Stoiber et al. 1986) (Delmelle et al. 1999; Stoiber et al. 1986) but few eruptions—there has been no major effusive activity since 1965 (Harris 2009)—although Masaya has a history of large basaltic Plinian eruptions (at 6 ka, 2.1 ka, 1.9 ka; (Pérez et al. 2020; Walker et al. 1993; Williams 1983). Presently, there is a lava lake at Masaya and evidence for a shallow subvolcanic reservoir (Aiuppa et al. 2018); petrological studies have reconstructed the equilibration pressure of the superhydrous melts responsible for explosive activity to below the seismic Moho (Pérez et al. 2020). The extension rate in Nicaragua has been estimated from the initiation of arc splitting and dating of volcanic products (Plank et al. 2002). The observed crustal thickness of 30–35 km greatly exceeds the ~ 10 km expected for the estimated 100-km extension over 15 Ma, suggesting that intrusive magmatism has infilled the space created by extension at a rate of 90–180 km^3/km/Ma (Morgan et al. 2008). Moreover, the estimated intrusive flux for Nicaragua is ~ 100 times the estimated volcanic output rate (Carr et al. 2003). This intrusive/extrusive ratio is much larger than the global average, which is ~ 5:1 (with a range of 1:1 to > 35:1) (Crisp 1984; White et al. 2006). Over the entire arc, regions of greatest extension also have the highest magma productivity and the strongest geochemical slab signature (as demonstrated by geochemical indices Ba/La and Yb/La (Burkart and Self 1985; Carr et al. 2003)). Nicaragua, specifically, has the largest magma productivity (intrusive and extrusive together), the highest rates of extension and slab flux and the strongest slab melting and source melting signals (Carr et al. 2003). Although it is unclear whether the large magma fluxes are a cause or an effect of upper plate extension, the large fluxes of intrusive magmas beneath the Managua graben allow ample opportunity for extensive second boiling and decompression degassing and production of a deep exsolved MVP. Venting of these deep-derived fluids advects heat to the shallow system and maintains a hot conduit.

Ambrym, a top-ranking volcanic open-vent outgasser (Figs. 1 and 4) located in the New Hebrides arc (Fig. 9b), is situated in the transition zone between a compressional regime in the central arc (Calmant et al. 2003) and an extensional regime in the south (Beier et al. 2018). The relative motion between the central and neighbouring northern and southern arc segments, respectively, is accommodated by dextral strike-slip zones (Pelletier et al. 1998). Ambrym, with its 12-km-wide caldera and the resurgent domes of Marum and Benbow, is located exactly at the transition from regional subsidence to strike-slip faulting (Picard et al. 1994). Changes in the stress field from compression to extension (plus rotation) has created a complex polybaric magmatic system (Beier et al. 2018), including accumulation of large intrusive volumes, crystallisation in shallow reservoirs and resulting large fluxes of exsolved volatiles that contribute to the persistent outgassing observed at Ambrym (Allard et al. 2016).

Etna has developed on the margin of the Hyblean plateau, the foreland to the Late Tertiary Maghrebian-Calabrian thrust belt, a compressional regime that started extending at ~ 0.5 Ma (Hirn et al. 1997; Laigle and Hirn 1999) (Fig. 9c). Crustal-scale normal faults imaged by reflection seismology extend over 20 km; their size, depth, location and evidence of activity suggests that these faults are the source of large earthquakes, which are associated with enhanced volcanism in time and space (Hirn et al. 1997). The specific location of Etna might be related to extension within a narrow zone of active normal faulting that stretches from the Hyblean Plateau in eastern Sicily to northern Calabria (Monaco et al. 1997). A high seismic velocity zone with a lateral dimension of ~ 6 km has been imaged beneath the summit at 9–18-km depth (Hirn et al. 1997). This body probably comprises cumulates produced from intrusive magmas, fragments of which are occasionally erupted as cognate xenoliths (Corsaro et al. 2014). This cumulate body likely contains significant volumes of volatile-rich melts generated through second boiling as well as regions dominated by an exsolved volatile phase. These fluids may mix with intruding basalts and ascend to shallow levels in the plumbing system shortly before eruptions, contributing to the large and persistent outgassing fluxes of Etna.

Persistently outgassing volcanoes in extensional (continental) regions include Erta Ale, Oldoinyo Lengai, Nyiragongo and Nyamuragira in the East African Rift and Erebus in the West Antarctic Rift system. A global link between outgassing and tectonics was suggested by Tamburello et al. (2018) to explain the distribution of high CO_2-emitting volcanic areas, which are focused in the extensional regions of arcs and in continental rifts. However, oceanic regions of extension are conspicuous for their lack of persistent volcanic outgassers. Iceland, for example, sits astride the Mid-Atlantic Ridge and has frequent eruptions but has no lava lakes or persistently outgassing conduits. Instead, frequent eruptions follow short periods of unrest (including increased outgassing) and return rapidly to closed-system behaviour once the eruption is over, although diffuse CO_2 degassing between eruptions may be linked to magma intrusions at depth (Ilyinskaya et al. 2018). In this respect, activity is more similar to other ocean islands such as Reunion, Galapagos or the Canary Islands, where sulphur-rich degassing occurs during, but not between, eruptions (Di Muro et al. 2016).

Depth-integrated magma degassing drives persistent outgassing and eruptive activity at open-vent volcanoes

A conclusion that can be drawn from the data and models presented above is that open-vent volcanoes may be thought of as predominantly gas, rather than lava, emitters. A corollary is that degassed magmas accumulate in the crust beneath open-vent volcanoes, thereby growing the crust endogenously. Open-vent volcanoes often occur in regions of crustal extension, which yield the accommodation space for large volumes of intruded magmas that ultimately form dry plutons once they crystallise, exsolve and lose their volatiles. Open-vent volcanoes are active for decades to millennia; their longevity may be controlled by the tectonics of the crust, which may cause different arc segments to 'switch on and off' over time (de Moor et al. 2017). Eruptions of open-vent volcanoes may be triggered by the ascent of segregated exsolved volatiles that flux through the shallow system or by volatile-rich melts that migrate rapidly from deeper levels in the crust, exsolving large volumes of volatiles as they ascend. Therefore, although traditionally it has been assumed that magma is the 'carrier' for advecting volatiles—requiring mass balance in the upper crust to account for open-vent outgassing fluxes (i.e. the convection model)—we have shown instead that large volumes of intruded magma at depth, stored at multiple levels throughout the crust, provide a potential source of segregated exsolved volatiles, which inevitably must contribute to the large outgassing fluxes at open-vent volcanoes. The framework model described here both removes the necessity for the volatiles to be supplied by continuous, large-vertical-scale bimodal flow and alleviates the space problem caused by the need to store large volumes of degassed magma within the shallowest parts of the crust.

For basalt-dominated open-vent volcanoes (Fig. 10a) with basalt or alkali basalt lava lakes or open vents (e.g. Stromboli, Yasur, Villarrica, Masaya, Fuego), volatiles may be delivered to the atmosphere through a combination of deep and shallow mechanisms, both consistent with the volcanic

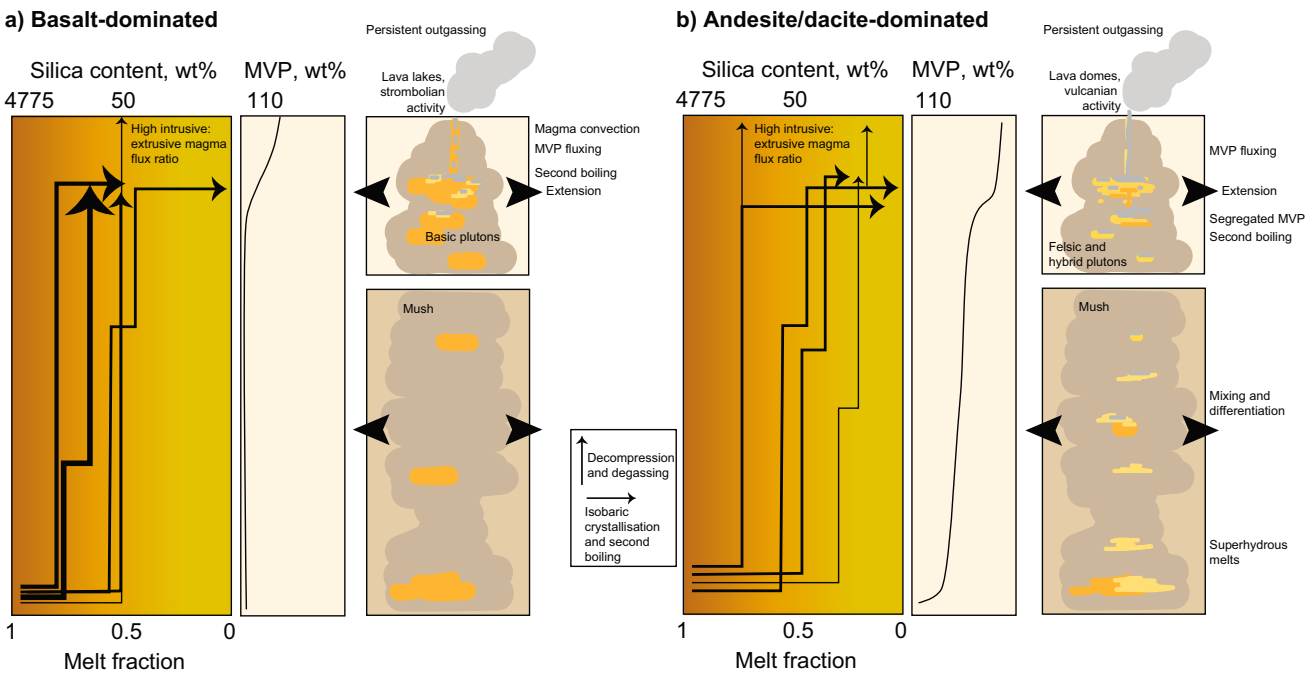

Fig. 10 Schematic diagram to illustrate the principal mechanisms of magma degassing at persistently active open-vent volcanoes. **a** At basalt-dominated volcanoes, magmas rise to shallow storage regions in the crust to form shallow basic plutons. Some magma may rise and convect in the conduit. The exsolved volatile phase that outgasses quasi-continuously from the volcano is sourced from a mix of deep (second boiling) and shallow (convective degassing) sources. Volcanic activity at these volcanoes is dominated by gas-driven strombolian activity and paroxysms, and there may be a semi-stable lava lake. **b** At andesite and dacite-dominated volcanoes, magmas undergo multi-level fractionation in the crust to form evolved melts which rise to shallow storage regions, exsolving a substantial exsolved volatile phase through second boiling. The persistent outgassing observed at these volcanoes is sourced principally from the second boiling process, which takes place during the solidification of hybrid and felsic plutons at depth. In both cases, magma intrusion and open-vent outgassing are promoted by crustal extension, which provides accommodation space for magma intrusion at depth and for the gravitational segregation of lower density exsolved volatile phases to the upper parts of the storage region. Deep generation of superhydrous melts may advect volatiles up to subvolcanic reservoirs

gas compositions observed at these volcanoes (Figs. 5, 6 and 7). Primitive basalts (which may be saturated in an exsolved volatile phase even at mantle depths in some cases) typically undergo ≥ 50% crystallisation in the crust to produce basaltic andesites or trachybasalts that dominate the shallow storage regions beneath these volcanoes. Exsolved volatiles generated through second boiling may migrate via capillary flow in crystal-rich mush in mid- and upper crustal magma storage regions, accumulating and segregating, perhaps giving rise to pockets of exsolved volatiles that may ascend rapidly to the surface and trigger paroxysms (Fig. 3). Primitive melts may be drawn into the conduit in the wake of these pockets of exsolved fluids. Although conduit convection may allow magmas to ascend to near atmospheric pressure, outgas and then sink, convection likely acts in tandem with the fluxing of deep-derived exsolved volatiles through the shallow conduit system. Together these processes may explain much of the outgassing volatile flux, as exemplified by Stromboli (Fig. 7b). The balance between convective degassing and deep MVP fluxing likely differs between volcanoes depending on both the depth of magma storage and crystallisation and the total volatile content of the magma. Volatile-rich magmas stored at relatively shallow depths are likely to produce a large volume of exsolved volatiles during even modest amounts of crystallisation. We note that this concept of exsolved volatiles being integrated over large depth ranges in the crust to supply open-vent outgassing is consistent with geochemical evidence from volcanic rocks that suggest that melt as well as crystals in magmas mingle over similarly large depth ranges (Cashman and Edmonds 2019; Ruth et al. 2018). A high magma intrusion rate will buffer the melt composition in the subvolcanic reservoir to produce monotonous erupted compositions and long-lived outgassing. The latent heating generated by extensive subvolcanic crystallisation combined with the rise of deep-derived exsolved volatiles (which efficiently advect heat) may produce sufficient heat to maintain hot conduits and lava lakes.

For intermediate composition open-vent volcanoes (dominated by andesites and dacites) (Fig. 10b) (e.g. Bagana, Soufrière Hills, Santiaguito, Anatahan), magma crystallisation over long timescales generates extensive regions of mush. The crystallisation of basalts at lower crustal depths may generate low viscosity hydrous or even 'superhydrous' basaltic andesite or andesite melts, as inferred for Kamchatka (Goltz et al. 2020). These melts may be further enriched in incompatible elements (including volatiles) upon mixing with highly evolved water-rich melt lenses in deep crustal mush. Petrological and experimental studies suggest mid-crustal water contents of 5–11 wt% in basaltic andesites from the Lesser Antilles (Edmonds et al. 2016; Melekhova et al. 2017). These volatile-rich melts may rise up to the mid and upper crust through percolation along grain boundaries or by the channelised reactive flow. The intrusion of volatile-rich basaltic andesite into shallower, more evolved mush-dominated reservoirs can induce partial melting, gas sparging (Bachmann and Bergantz 2006) and/or trigger gravitational destabilisation or eruption (Christopher et al. 2015). The volatile-rich melts may generate substantial fractions of exsolved volatiles in mid and upper crustal mush-dominated reservoirs, which may accumulate and segregate from their rhyolitic melt lenses over millennia. These volatile-rich lenses may be later tapped by eruptions and drive persistent and long-lived volcanic outgassing. Importantly, bimodal flow and convective degassing are precluded in volcanoes dominated by crystal-rich, hydrous intermediate composition magma because of extensive decompression-induced crystallisation and resulting high bulk viscosity of the magma. In these systems, persistent degassing requires volatile migration that is independent of magma migration.

A generic model for the degassing regime at open-vent volcanoes brings together our understanding of magmatic crystallisation, mixing and storage processes with our observations of volcanic gas flux and composition at open-vent volcanoes. Intrusive, unerupted magmas crystallising at a range of crustal depths generate a substantial exsolved volatile phase, which is fluxed into the overlying system and up through conduits. Volatile fluxing advects heat and brings with it small volumes of primitive melts that replenish the melt resident in the shallow magma storage and conduit systems. Although basalt-dominated reservoirs may also experience subsidiary convection, convection is unlikely in more evolved, mush-dominated magmatic systems, where the outgassing flux will instead be dominated by the fluxing of a deep-derived MVP generated through second boiling. In this model, large bodies of crystal-rich mush generated through extensive crystallisation remain in situ at a range of depths, with no requirement for magmas to convect to atmospheric pressure and back down again. Volcanic gases emitted from these volcanoes are the integrated products of the degassing of melts at a range of crustal depths that have undergone various degrees of crystallisation and mixing.

Conclusions

1. Open-vent volcanoes produce large outgassing fluxes, much greater than can be supplied by erupting magmas. Open-vent volcanoes may be thought of as gas vents connecting the mantle and/or crust to the atmosphere.
2. Open-vent volcanoes produce explosive and gas-rich eruptions, e.g. violent strombolian, vulcanian and paroxysms, that are triggered by the rise of volatile-rich melts and/or fluxing of segregated exsolved volatiles from deeper mush-dominated magma storage regions.

3. Volcanic gas compositions at open-vent volcanoes are likely derived from a mixture of exsolved volatile produced from decompressional degassing, whereby magmas degas during their ascent to atmospheric pressure, and isobaric (or polybaric) second boiling in the crust, which generates a substantial volume of exsolved volatiles during crystallisation.
4. High fluxes of deep exsolved volatiles are sourced from the second boiling of intrusive magmas in the mid to lower crust. These deep-derived exsolved volatiles flux through shallow volcanic systems, advecting heat, sustaining persistent degassing and triggering eruptions. These processes are particularly important for more evolved, water-rich volcanic systems.
5. Bimodal flow and magma convection may operate in low viscosity basaltic systems, which brings magma up to near atmospheric pressure to outgas and then sink back down, but this mechanism acts in tandem with fluxing by a deeper-derived volatile phase. Convection is not likely to be important in more water-rich, more evolved volcanic systems, due to the extensive degassing-induced crystallisation in the conduit, which will stall magma return flow by viscous inhibition.
6. Intrusion and degassing of magma into the crust beneath open-vent volcanoes is accommodated by extensional tectonics and the extension plays a role in allowing exsolved fluids to migrate up to the shallow volcanic systems. The location and longevity of open-vent volcanic outgassing and activity are likely controlled by tectonics.
7. Open-vent volcanic outgassing is an integrated product of the degassing of a vertically-protracted magmatic storage and transport system, not merely a shallow magma reservoir. A great challenge for volcano monitoring in the future will be to detect and understand both geochemical and geophysical signals from the mid and lower crust to enhance eruption forecasting.
8. Accurate measurements of outgassing volatile and magma fluxes from individual volcanoes and from volcanic regions may greatly improve existing estimates of intrusive/extrusive magma fluxes and their link to tectonics.

Supplementary Information The online version contains supplementary material available at https://doi.org/10.1007/s00445-021-01522-8.

Acknowledgements We thank Nicole Métrich and Andrew Harris for their editorial handling of our manuscript, as well as John Stix and two other anonymous reviewers.

Funding This work was supported by the Natural Environment Research Council COMET program. K.V.C. is supported by an AXA Professorial Fellowship.

Data availability All data generated in this paper through modelling are available in the Supplementary Material.

Declarations

Conflict of interest The authors declare no competing interests.

References

Aiuppa A (2009) Degassing of halogens from basaltic volcanism: insights from volcanic gas observations. Chem Geol 263:99–109

Aiuppa A, Federico C, Paonita A, Pecoraino G, Valenza M (2002) S, Cl and F degassing as an indicator of volcanic dynamics: the 2001 eruption of Mount Etna. Geophys Res Lett 29:54-51–54-54

Aiuppa A, Bellomo S, D'Alessandro W, Federico C, Ferm M, Valenza M (2004) Volcanic plume monitoring at Mount Etna by diffusive (passive) sampling. J Geophys Res-Atmos 109

Aiuppa A, Federico C, Giudice G, Gurrieri S, Liuzzo M, Shinohara H, Favara R, Valenza MJJ (2006) Rates of carbon dioxide plume degassing from Mount Etna volcano. Journal of Geophysical Research: Solid Earth 111(B9)

Aiuppa A, Moretti R, Federico C, Giudice G, Gurrieri S, Liuzzo M, Papale P, Shinohara H, Valenza M (2007) Forecasting Etna eruptions by real-time observation of volcanic gas composition. Geology 35:1115–1118

Aiuppa A, Giudice G, Gurrieri S, Liuzzo M, Burton M, Caltabiano T, McGonigle A, Salerno G, Shinohara H, Valenza M (2008) Total volatile flux from Mount Etna. Geophys Res Lett:35

Aiuppa A, Bertagnini A, Métrich N, Moretti R, Di Muro A, Liuzzo M, Tamburello G (2010) A model of degassing for Stromboli volcano. Earth Planet Sci Lett 295:195–204

Aiuppa A, Robidoux P, Fischer T (2015) Along-arc and inter-arc variations in volcanic gas CO2/S signature, *in* Proceedings EGU General Assembly Conference Abstracts, Volume 17, p. 3773

Aiuppa A, Bitetto M, Francofonte V, Velasquez G, Parra CB, Giudice G, Liuzzo M, Moretti R, Moussallam Y, Peters N (2017) A CO2-gas precursor to the March 2015 Villarrica volcano eruption. Geochem Geophys Geosyst 18:2120–2132

Aiuppa A, de Moor JM, Arellano S, Coppola D, Francofonte V, Galle B, Giudice G, Liuzzo M, Mendoza E, Saballos AJG (2018) Tracking formation of a lava lake from ground and space: Masaya volcano (Nicaragua), 2014–2017. Geophys Geosyst 19:496–515

Allard P (1997) Endogenous magma degassing and storage at Mount Etna. Geophys Res Lett 24:2219–2222

Allard P (2010) A CO2-rich gas trigger of explosive paroxysms at Stromboli basaltic volcano, Italy. J Volcanol Geotherm Res 189:363–374

Allard P, Carbonnelle J, Metrich N, Loyer H, Zettwoog P (1994) Sulphur output and magma degassing budget of Stromboli volcano. Nature 368:326

Allard P, Burton M, Mure F (2005) Spectroscopic evidence for a lava fountain driven by previously accumulated magmatic gas. Nature 433:407–410

Allard P, Behncke B, D'Amico S, Neri M, Gambino S (2006) Mount Etna 1993–2005: anatomy of an evolving eruptive cycle. Earth Sci Rev 78:85–114

Allard P, Aiuppa A, Burton M, Caltabiano T, Federico C, Salerno G, La Spina A (2008) Crater gas emissions and the magma feeding system of Stromboli volcano. Learn Stromboli: AGU Geophys Monogr Ser 182:65–80

Allard P, Aiuppa A, Bani P, Métrich N, Bertagnini A, Gauthier PJ, Shinohara H, Sawyer G, Parello F, Bagnato E, Pelletier B (2016) Prodigious emission rates and magma degassing budget of major, trace and radioactive volatile species from Ambrym basaltic volcano, Vanuatu island Arc. Journal of volcanology and geothermal research. 322:119–43

Alletti M, Baker DR, Scaillet B, Aiuppa A, Moretti R, Ottolini L (2009) Chlorine partitioning between a basaltic melt and H2O–CO2 fluids at Mount Etna. Chem Geol 263:37–50

Anderson AT (1975) Some basaltic and andesitic gases. Rev Geophys Space Phys 13:37–55

Andres R, Kasgnoc A (1998) A time-averaged inventory of subaerial volcanic sulfur emissions. J Geophys Res-Atmos (1984–2012 103:25251–25261

Andres R, Rose WI, Kyle P, DeSilva S, Francis P (1991) Excessive sulfur dioxide emissions from Chilean volcanoes. J Volcanol Geotherm Res 46:323–329

Arciniega-Ceballos A, Chouet B, Dawson P, Asch G (2008) Broadband seismic measurements of degassing activity associated with lava effusion at Popocatépetl Volcano, Mexico. J Volcanol Geotherm Res 170:12–23

Arellano S, Galle B, Apaza F, Avard G, Barrington C, Bobrowski N, Bucarey C, Burbano V, Burton M, Chacón Z, Chigna G (2021) Synoptic analysis of a decade of daily measurements of SO2 emission in the troposphere from volcanoes of the global ground-based Network for Observation of Volcanic and Atmospheric Change. Earth System Science Data. 13(3):1167–88

Aso N, Tsai VC (2014) Cooling magma model for deep volcanic long-period earthquakes. J Geophys Res Solid Earth 119:8442–8456

Aster R, Zandomeneghi D, Mah S, McNamara S, Henderson DB, Knox H, Jones K (2008) Moment tensor inversion of very long period seismic signals from Strombolian eruptions of Erebus Volcano. Journal of Volcanology and Geothermal Research. 177(3):635–47

Bachmann O, Bergantz GW (2004) On the origin of crystal-poor rhyolites: extracted from batholithic crystal mushes. J Petrol 45:1565–1582

Bachmann O, Bergantz G (2006) Gas percolation in upper-crustal silicic crystal mushes as a mechanism for upward heat advection and rejuvenation of near-solidus magma bodies. J Volcanol Geotherm Res 149:85–102

Bachmann O, Miller C, De Silva S (2007) The volcanic–plutonic connection as a stage for understanding crustal magmatism. J Volcanol Geotherm Res 167:1–23

Bani P, Lardy M (2007) Sulphur dioxide emission rates from Yasur volcano, Vanuatu archipelago. Geophysical Research Letters 34(20)

Bani P, Oppenheimer C, Tsanev VI, Carn SA, Cronin SJ, Crimp R, Calkins JA, Charley D, Lardy M, Roberts TR (2009) Surge in sulphur and halogen degassing from Ambrym volcano, Vanuatu. Bull Volcanol 71:1159–1168

Bani P, Oppenheimer C, Allard P, Shinohara H, Tsanev V, Carn S, Lardy M, Garaebiti E (2012) First estimate of volcanic SO 2 budget for Vanuatu island arc. J Volcanol Geotherm Res 211:36–46

Barth A, Edmonds M, Woods A (2019) Valve-like dynamics of gas flow through a packed crystal mush and cyclic strombolian explosions. Sci Rep 9:821

Beckett F, Mader H, Phillips J, Rust A, Witham F (2011) An experimental study of low-Reynolds-number exchange flow of two Newtonian fluids in a vertical pipe. J Fluid Mech 682:652

Beckett F, Burton M, Mader H, Phillips J, Polacci M, Rust A, Witham F (2014) Conduit convection driving persistent degassing at basaltic volcanoes. J Volcanol Geotherm Res 283:19–35

Beier C, Brandl PA, Lima SM, Haase KM (2018) Tectonic control on the genesis of magmas in the New Hebrides arc (Vanuatu). Lithos 312:290–307

Belien IB, Cashman KV, Rempel AW (2010) Gas accumulation in particle-rich suspensions and implications for bubble populations in crystal-rich magma. Earth Planet Sci Lett 297:133–140

Bertagnini A, Métrich N, Landi P, Rosi M (2003) Stromboli volcano (Aeolian Archipelago, Italy): An open window on the deep-feeding system of a steady state basaltic volcano. Journal of Geophysical Research: Solid Earth 108(B7)

Bertagnini A, Di Roberto A, Pompilio M (2011) Paroxysmal activity at Stromboli: lessons from the past. Bull Volcanol 73:1229–1243

Blackburn E, Wilson L, Sparks RSJ (1976) Mechanisms and dynamics of strombolian activity. J Geol Soc 132:429–440

Blundy J, Cashman KV, Rust A, Witham F (2010) A case for CO 2-rich arc magmas. Earth Planet Sci Lett 290:289–301

Bluth GJ, Rose WI (2004) Observations of eruptive activity at Santiaguito volcano, Guatemala. J Volcanol Geotherm Res 136:297–302

Botcharnikov R, Behrens H, Holtz F, Koepke J, Sato H (2004) Sulfur and chlorine solubility in Mt. Unzen rhyodacitic melt at 850 C and 200 MPa. Chem Geol 213:207–225

Botcharnikov R, Holtz F, Behrens H (2015) Solubility and fluid–melt partitioning of H2O and Cl in andesitic magmas as a function of pressure between 50 and 500 MPa. Chem Geol 418:117–131

Bouche E, Vergniolle S, Staudacher T, Nercessian A, Delmont JC, Frogneux M, Cartault F, Le Pichon A (2010) The role of large bubbles detected from acoustic measurements on the dynamics of Erta 'Ale lava lake (Ethiopia). Earth Planet Sci Lett 295:37–48

Bultitude RJ (1981) Literature search for pre-1945 sightings of volcanoes and their activity on Bougainville Island. InCooke-Ravian volume of volcanological papers. Geological Survey of Papua New Guinea, Port Moresby, Memoir 10:227–242

Burkart B, Self S (1985) Extension and rotation of crustal blocks in northern Central America and effect on the volcanic arc. Geology. 13(1):22–6

Burton M, Allard P, Mure F, Oppenheimer C (2003) FTIR remote sensing of fractional magma degassing at Mount Etna, Sicily. Geol Soc Lond Spec Publ 213:281–293

Burton M, Allard P, Muré F, La Spina A (2007) Magmatic gas composition reveals the source depth of slug-driven Strombolian explosive activity. Science 317:227–230

Calmant S, Pelletier B, Lebellegard P, Bevis M, Taylor FW, Phillips DA (2003) New insights on the tectonics along the New Hebrides subduction zone based on GPS results. Journal of Geophysical Research: Solid Earth 108(B6)

Caltabiano T, Romano R, Budetta G (1994) SO2 flux measurements at Mount Etna (Sicily). J Geophys Res-Atmos (1984–2012 99:12809–12819

Calvari S, Spampinato L, Bonaccorso A, Oppenheimer C, Rivalta E, Boschi E (2011) Lava effusion—a slow fuse for paroxysms at Stromboli volcano? Earth Planet Sci Lett 301:317–323

Candela PA (1997) A review of shallow, ore-related granites: textures, volatiles, and ore metals. J Petrol 38:1619–1633

Caracciolo A, Gurioli L, Marianelli P, Bernard J, Harris A (2021) Textural and chemical features of a "soft" plug emitted during Strombolian explosions: a case study from Stromboli volcano. Earth Planet Sci Lett 559:116761

Cardoso SS, Woods AW (1999) On convection in a volatile-saturated magma. Earth Planet Sci Lett 168:301–310

Caricchi L, Sheldrake TE, Blundy J (2018) Modulation of magmatic processes by CO 2 flushing. Earth Planet Sci Lett 491:160–171

Carn S, Clarisse L, Prata A (2016) Multi-decadal satellite measurements of global volcanic degassing. J Volcanol Geotherm Res 311:99–134

Carn S, Fioletov V, McLinden C, Li C, Krotkov N (2017) A decade of global volcanic SO 2 emissions measured from space. Sci Rep 7:44095

Carr M, Feigenson M, Patino L, Walker J (2003) Volcanism and geochemistry in Central America: progress and problems. Geophys Monogr Am Geophys Union 138:153–174

Cashman KV (2004) Volatile controls on magma ascent and eruption. The State of the Planet: Frontiers and Challenges in Geophysics. 150:109–24

Cashman K, Blundy J (2000) Degassing and crystallization of ascending andesite and dacite. Philosophical Transactions of the Royal Society of London. Ser A Math Phys Eng Sci 358:1487–1513

Cashman KV, Edmonds M (2019) Mafic glass compositions: a record of magma storage conditions, mixing and ascent. Phil Trans R Soc A 377:20180004

Cashman KV, Sparks RS (2013) How volcanoes work: A 25 year perspective. GSA bulletin. 125(5–6):664–90

Cashman KV, Sparks RSJ, Blundy JD (2017) Vertically extensive and unstable magmatic systems: a unified view of igneous processes. Science 355:eaag3055

Chouet BA (1996) Long-period volcano seismicity: its source and use in eruption forecasting. Nature 380:309–316

Chouet B, Saccorotti G, Dawson P, Martini M, Scarpa R, De Luca G, Milana G, Cattaneo M (1999) Broadband measurements of the sources of explosions at Stromboli Volcano, Italy. Geophys Res Lett 26:1937–1940

Chouet B, Dawson P, Arciniega-Ceballos A (2005) Source mechanism of Vulcanian degassing at Popocatépetl Volcano, Mexico, determined from waveform inversions of very long period signals. Journal of Geophysical Research: Solid Earth 110(B7)

Christopher T, Edmonds M, Humphreys MC, Herd RA (2010) Volcanic gas emissions from Soufrière Hills Volcano, Montserrat 1995–2009, with implications for mafic magma supply and degassing. Geophysical Research Letters 37(19)

Christopher T, Blundy J, Cashman K, Cole P, Edmonds M, Smith P, Sparks R, Stinton A (2015) Crustal-scale degassing due to magma system destabilization and magma-gas decoupling at Soufrière Hills Volcano, Montserrat. Geochem Geophys Geosyst

Clémente B, Scaillet B, Pichavant M (2004) The solubility of sulphur in hydrous rhyolitic melts. J Petrol 45:2171–2196

Colombier M, Wadsworth FB, Scheu B, Vasseur J, Dobson KJ, Cáceres F, Allabar A, Marone F, Schlepütz CM, Dingwell DB (2020) In situ observation of the percolation threshold in multiphase magma analogues. Bulletin of volcanology. 82(4):1–5

Collombet M, Burgisser A, Colombier M, Gaunt E (2021) Evidence for deep gas loss in open volcanic systems. Bulletin of Volcanology. 83(2):1–6

Coppola D, Laiolo M, Massimetti F, Cigolini C (2019) Monitoring endogenous growth of open-vent volcanoes by balancing thermal and SO 2 emissions data derived from space. Sci Rep 9:1–12

Corsaro RA, Rotolo SG, Cocina O, Tumbarello G (2014) Cognate xenoliths in Mt. Etna lavas: witnesses of the high-velocity body beneath the volcano. Bull Volcanol 76:772

Crisp JA (1984) Rates of magma emplacement and volcanic output. J Volcanol Geotherm Res 20:177–211

de Moor JM, Aiuppa A, Avard G, Wehrmann H, Dunbar N, Muller C, Tamburello G, Giudice G, Liuzzo M, Moretti R (2016) Turmoil at Turrialba Volcano (Costa Rica): degassing and eruptive processes inferred from high-frequency gas monitoring. J Geophys Res Solid Earth 121:5761–5775

de Moor J, Kern C, Avard G, Muller C, Aiuppa A, Saballos A, Ibarra M, LaFemina P, Protti M, Fischer T (2017) A new sulfur and carbon degassing inventory for the Southern Central American Volcanic Arc: the importance of accurate time-series data sets and possible tectonic processes responsible for temporal variations in arc-scale volatile emissions. Geochem Geophys Geosyst 18:4437–4468

Degruyter W, Parmigiani A, Huber C, Bachmann O (2019) How do volatiles escape their shallow magmatic hearth? Philosophical Transactions of the Royal Society A. 377(2139):20180017

DeGraffenried RL, Larsen JF, Graham NA, Cashman KV (2019) The influence of phenocrysts on degassing in crystalbearing magmas with rhyolitic groundmass melts. Geophysical Research Letters. 46(10):5127–36

Del Bello E, Lane SJ, James MR, Llewellin EW, Taddeucci J, Scarlato P, Capponi A (2015) Viscous plugging can enhance and modulate explosivity of strombolian eruptions. Earth Planet Sci Lett 423:210–218

Delmelle P, Baxter P, Beaulieu A, Burton M, Francis P, Garcia-Alvarez J, Horrocks L, Navarro M, Oppenheimer C, Rothery D (1999) Integrated geochemical, geophysical, and petrological studies illuminate magmatic processes at Masaya volcano, Nicaragua. EOS Submitted

Di Muro A, Métrich N, Allard P, Aiuppa A, Burton M, Galle B, Staudacher T (2016) Magma degassing at Piton de la Fournaise volcano, Active Volcanoes of the Southwest Indian Ocean. Springer, pp 203–222

Dingwell DB (1996) Volcanic dilemma: flow or blow? Science 273:1054

Edmonds M, Herd RA (2007) A volcanic degassing event at the explosive-effusive transition. Geophysical Research Letters 34(21)

Edmonds M, Wallace PJ (2017) Volatiles and exsolved vapor in volcanic systems. Elements 13:29–34

Edmonds M, Woods AW (2018) Exsolved volatiles in magma reservoirs. J Volcanol Geotherm Res 368:13–30

Edmonds M, Pyle D, Oppenheimer C (2001) A model for degassing at the Soufrière Hills Volcano, Montserrat, West Indies, based on geochemical data. Earth Planet Sci Lett 186:159–173

Edmonds M, Pyle D, Oppenheimer C (2002) HCl emissions at Soufrière Hills Volcano, Montserrat, West Indies, during a second phase of dome building: November 1999 to October 2000. Bull Volcanol 64:21–30

Edmonds M, Aiuppa A, Humphreys M, Moretti R, Giudice G, Martin RS, Herd RA, Christopher T (2010) Excess volatiles supplied by mingling of mafic magma at an andesite arc volcano. Geochemistry, Geophysics, Geosystems 11(4)

Edmonds M, Humphreys MC, Hauri EH, Herd RA, Wadge G, Rawson H, Ledden R, Plail M, Barclay J, Aiuppa A (2014) Pre-eruptive vapour and its role in controlling eruption style and longevity at Soufrière Hills Volcano. Geol Soc Lond Mem 39:291–315

Edmonds M, Kohn S, Hauri E, Humphreys M, Cassidy M (2016) Extensive, water-rich magma reservoir beneath southern Montserrat. Lithos 252:216–233

Fioletov VE, McLinden CA, Krotkov N, Li C, Joiner J, Theys N, Carn S, Moran MD (2016) A global catalogue of large SO 2 sources and emissions derived from the Ozone Monitoring Instrument. Atmos Chem Phys 16

Fischer TP (2008) Fluxes of volatiles (H2O, CO2, N2, Cl, F) from arc volcanoes. Geochem J 42:21–38

Foley SF, Fischer TP (2017) An essential role for continental rifts and lithosphere in the deep carbon cycle. Nat Geosci 10:897

Francis P, Oppenheimer C, Stevenson D (1993) Endogenous growth of persistently active volcanoes. Nature 366:554–557
Gaunt HE, Sammonds PR, Meredith PG, Smith R, Pallister JS (2014) Pathways for degassing during the lava dome eruption of Mount St. Helens 2004–2008. Geology 42:947–950
Ghiorso M, Gualda G (2015a) An H2O–CO2 mixed fluid saturation model compatible with rhyolite-MELTS. Contrib Mineral Petrol 169:1–30
Ghiorso MS, Gualda GA (2015b) An H 2 O–CO 2 mixed fluid saturation model compatible with rhyolite-MELTS. Contrib Mineral Petrol 169:53
Giachetti T, Gonnermann HM, Gardner JE, Burgisser A, Hajimirza S, Earley TC, Truong N, Toledo P (2019) Bubble coalescence and percolation threshold in expanding rhyolitic magma. Geochemistry, Geophysics, Geosystems. 20(2):1054–74
Giggenbach W (1992) Isotopic shifts in waters from geothermal and volcanic systems along convergent plate boundaries and their origin. Earth Planet Sci Lett 113:495–510
Giggenbach W (1996) Chemical composition of volcanic gases, monitoring and mitigation of volcano hazards. Springer, pp 221–256
Giordano D, Russell JK, Dingwell DB (2008) Viscosity of magmatic liquids: a model. Earth Planet Sci Lett 271:123–134
Goltz AE, Krawczynski MJ, Gavrilenko M, Gorbach NV, Ruprecht P (2020) Evidence for superhydrous primitive arc magmas from mafic enclaves at Shiveluch volcano, Kamchatka. Contrib Mineral Petrol 175:1–26
Gonnermann HM, Manga M (2003) Explosive volcanism may not be an inevitable consequence of magma fragmentation. Nature 426:432–435
Gurioli L, Harris A, Houghton B, Polacci M, Ripepe M (2008) Textural and geophysical characterization of explosive basaltic activity at Villarrica volcano. J Geophys Res Solid Earth 113
Gurioli L, Colo' L, Bollasina A, Harris AJ, Whittington A, Ripepe M (2014) Dynamics of Strombolian explosions: inferences from field and laboratory studies of erupted bombs from Stromboli volcano. J Geophys Res Solid Earth 119:319–345
Hammouya G, Allard P, Jean-Baptiste P, Parello F, Semet M, Young S (1998) Pre-and syn-eruptive geochemistry of volcanic gases from Soufriere Hills of Montserrat, West Indies. Geophys Res Lett 25:3685–3688
Harris AJ (2008) Modeling lava lake heat loss, rheology, and convection. Geophysical Research Letters 35(7)
Harris A (2009) The pit-craters and pit-crater-filling lavas of Masaya volcano. Bull Volcanol 71:541–558
Harris AJ, Carniel R, Jones J (2005) Identification of variable convective regimes at Erta Ale Lava Lake. J Volcanol Geotherm Res 142:207–223
Hautmann S, Witham F, Christopher T, Cole P, Linde AT, Sacks IS, Sparks RSJ (2014) Strain field analysis on Montserrat (WI) as tool for assessing permeable flow paths in the magmatic system of Soufrière Hills Volcano. Geochem Geophys Geosyst 15:676–690
Herd RA, Edmonds M, Bass VA (2005) Catastrophic lava dome failure at Soufrière Hills volcano, Montserrat, 12–13 July 2003. J Volcanol Geotherm Res 148:234–252
Hidayat D, Chouet B, Voight B, Dawson P, Ratdomopurbo A (2002) Source mechanism of very-long-period signals accompanying dome growth activity at Merapi volcano, Indonesia. Geophys Res Lett 29:33-31–33-34
Hirn A, Nicolich R, Gallart J, Laigle M, Cernobori L, ETNASEIS Scientific Group (1997) Roots of Etna volcano in faults of great earthquakes. Earth and Planetary Science Letters 148(1-2):171–91
Hoff R, Millan M (1981) Remote SO2 mass flux measurements using COSPEC. J Air Pollut Control Assoc 31:381–384
Holland AP, Watson IM, Phillips JC, Caricchi L, Dalton MP (2011) Degassing processes during lava dome growth: insights from Santiaguito lava dome, Guatemala. J Volcanol Geotherm Res 202:153–166
Huber C, Bachmann O, Manga M (2010) Two competing effects of volatiles on heat transfer in crystal-rich magmas: thermal insulation vs defrosting. J Petrol 51:847–867
Huppert HE, Hallworth MA (2007) Bi-directional flows in constrained systems. J Fluid Mech 578:95
Hurwitz S, Navon O (1994) Bubble nucleation in rhyolitic melts: Experiments at high pressure, temperature, and water content. Earth and Planetary Science Letters. 122(3–4):267–80
Ilanko T, Pering TD, Wilkes TC, Woitischek J, D'Aleo R, Aiuppa A, McGonigle AJ, Edmonds M, Garaebiti E (2020) Ultraviolet camera measurements of passive and explosive (Strombolian) sulphur dioxide emissions at yasur volcano, Vanuatu. Remote Sens 12:2703
Ilyinskaya E, Mobbs S, Burton R, Burton M, Pardini F, Pfeffer MA, Purvis R, Lee J, Bauguitte S, Brooks B, Colfescu I (2018) Globally significant CO2 emissions from Katla, a subglacial volcano in Iceland. Geophysical Research Letters. 45(19):10–332
Iverson RM (2008) Dynamics of seismogenic volcanic extrusion resisted by a solid surface plug, Mount St. Helens, 2004-2005: US Geological Survey, 2330-7102
James MR, Lane SJ, Chouet BA (2006) Gas slug ascent through changes in conduit diameter: Laboratory insights into a volcano-seismic source process in low-viscosity magmas. Journal of Geophysical Research: Solid Earth 111(B5).
Jaupart C, Vergniolle S (1988) Laboratory models of Hawaiian and Strombolian eruptions. Nature 331:58–60
Jaupart C, Vergniolle S (1989) The generation and collapse of a foam layer at the roof of a basaltic magma chamber. J Fluid Mech 203:347–380
Johnson JB, Lyons JJ, Andrews BJ, Lees JM (2014) Explosive dome eruptions modulated by periodic gas-driven inflation. Geophys Res Lett 41:6689–6697
Johnson JB, Watson LM, Palma JL, Dunham EM, Anderson JF (2018) Forecasting the eruption of an open-vent volcano using resonant infrasound tones. Geophysical Research Letters. 45(5):2213–20
Kazahaya K, Shinohara H, Saito G (1994) Excessive degassing of Izu-Oshima volcano: magma convection in a conduit. Bull Volcanol 56:207–216
Kazahaya K, Shinohara H, Uto K, Odai M, Nakahori Y, Mori H, Iino H, Miyashita M, Hirabayashi J (2004) Gigantic SO2 emission from Miyakejima volcano, Japan, caused by caldera collapse. Geology 32:425–428
Kazahaya R, Mori T, Takeo M, Ohminato T, Urabe T, Maeda Y (2011) Relation between single very-long-period pulses and volcanic gas emissions at Mt. Asama, Japan. Geophysical research letters 38(11)
Kilinc I, Burnham C (1972) Partitioning of chloride between a silicate melt and coexisting aqueous phase from 2 to 8 kilobars. Econ Geol 67:231–235
Koulakov I, Gordeev EI, Dobretsov NL, Vernikovsky VA, Senyukov S, Jakovlev A, Jaxybulatov K (2013) Rapid changes in magma storage beneath the Klyuchevskoy group of volcanoes inferred from time-dependent seismic tomography. Journal of Volcanology and Geothermal Research. 263:75–91
Koulakov I, Smirnov S, Gladkov V, Kasatkina E, West M, El Khrepy S, Al-Arifi N (2018) Causes of volcanic unrest at Mt. Spurr in 2004–2005 inferred from repeated tomography. Sci Rep 8:1–7
Kremers S, Lavallée Y, Hanson J, Hess KU, Chevrel MO, Wassermann J, Dingwell DB (2012) Shallow magma-mingling-driven Strombolian eruptions at Mt. Yasur volcano, Vanuatu. Geophys Res Lett 39

Kuznetsov PY, Koulakov I, Jakovlev A, Abkadyrov I, Deev E, Gordeev EI, Senyukov S, El Khrepy S, Al Arifi N (2017) Structure of volatile conduits beneath Gorely volcano (Kamchatka) revealed by local earthquake tomography. Geosciences 7:111

La Felice S, Landi P (2011) The 2009 paroxysmal explosions at Stromboli (Italy): magma mixing and eruption dynamics. Bull Volcanol 73:1147–1154

Lages J, Liuzzo M, Giudice G, Aiuppa A, Chacón Z, Burbano V, Meza L, Rizzo A, Bitetto M, López C (2018) Volcanic CO2 and SO2 emissions along the Colombia Arc Segment (Northern Volcanic Zone), *in* Proceedings EGU General Assembly Conference Abstracts, p. 1301

Laigle M, Hirn A (1999) Explosion-seismic tomography of a magmatic body beneath Etna: Volatile discharge and tectonic control of volcanism. Geophysical research letters. 26(17):2665–8

Lamb OD, Lamur A, Díaz-Moreno A, De Angelis S, Hornby AJ, von Aulock FW, Kendrick JE, Wallace PA, Gottschämmer E, Rietbrock A (2019) Disruption of long-term effusive-explosive activity at Santiaguito, Guatemala. Front Earth Sci 6:253

Landi P, Metrich N, Bertagnini A, Rosi M (2004) Dynamics of magma mixing and degassing recorded in plagioclase at Stromboli (Aeolian Archipelago, Italy). Contrib Mineral Petrol 147:213–227

Lautze NC, Houghton BF (2007) Linking variable explosion style and magma textures during 2002 at Stromboli volcano, Italy. Bull Volcanol 69:445–460

Lejeune AM, Richet P (1995) Rheology of crystal-bearing silicate melts: An experimental study at high viscosities. J Geophys Res Solid Earth 100:4215–4229

Lesne P, Kohn SC, Blundy J, Witham F, Botcharnikov RE, Behrens H (2011) Experimental simulation of closed-system degassing in the system basalt–H2O–CO2–S–Cl. Journal of Petrology 52(9):1737–62

Lev E, Ruprecht P, Oppenheimer C, Peters N, Patrick M, Hernández PA, Spampinato L, Marlow J (2019) A global synthesis of lava lake dynamics. J Volcanol Geotherm Res 381:16–31

Linde AT, Sacks S, Hidayat D, Voight B, Clarke A, Elsworth D, Mattioli G, Malin P, Shalev E, Sparks S, Widiwijayanti C (2010) Vulcanian explosion at Soufrière Hills Volcano, Montserrat on March 2004 as revealed by strain data. Geophysical Research Letters 37(19)

Lindoo A, Larsen JF, Cashman KV, Oppenheimer J (2017) Crystal controls on permeability development and degassing in basaltic andesite magma. Geology. 45(9):831–4

Lindoo A, Larsen JF, Cashman KV, Dunn AL, Neill OK (2016) An experimental study of permeability development as a function of crystal-free melt viscosity. Earth and Planetary Science Letters. 435:45–54

Lipman PW, Banks NG, Rhodes JM (1985) Degassing-induced crystallization of basaltic magma and effects on lava rheology. Nature 317:604–607

Liu EJ, Aiuppa A, Alan A, Arellano S, Bitetto M, Bobrowski N, Carn S, Clarke R, Corrales E, de Moor JM (2020a) Aerial strategies advance volcanic gas measurements at inaccessible, strongly degassing volcanoes. Sci Adv 6:eabb9103

Liu EJ, Cashman KV, Miller E, Moore H, Edmonds M, Kunz BE, Jenner F, Chigna G (2020b) Petrologic monitoring at Volcán de Fuego, Guatemala. J Volcanol Geotherm Res 405:107044

Londoño JM, Kumagai H (2018) 4D seismic tomography of Nevado del Ruiz Volcano, Colombia, 2000–2016. J Volcanol Geotherm Res 358:105–123

Lyons JJ, Waite GP, Rose WI, Chigna G (2010) Patterns in open vent, strombolian behavior at Fuego volcano, Guatemala, 2005–2007. Bull Volcanol 72:1

McCormick Kilbride BT, Mulina K, Wadge G, Johnson R, Itikarai I, Edmonds M (2019) Multi-year satellite observations of sulfur dioxide gas emissions and lava extrusion at Bagana volcano, Papua New Guinea. Front Earth Sci 7:9

McCormick BT, Edmonds M, Mather TA, Carn SA (2012) First synoptic analysis of volcanic degassing in Papua New Guinea. Geochemistry, Geophysics, Geosystems 13(3)

McGonigle A, Oppenheimer C, Tsanev V, Saunders S, Mulina K, Tohui S, Bosco J, Nahou J, Kuduon J, Taranu F (2004) Sulphur dioxide fluxes from Papua New Guinea's volcanoes. Geophys Res Lett 31

McNutt SR, Roman DC (2015) Volcanic seismicity, The Encyclopedia of Volcanoes. Elsevier, pp 1011–1034

Melekhova E, Blundy J, Martin R, Arculus R, Pichavant M (2017) Petrological and experimental evidence for differentiation of water-rich magmas beneath St. Kitts, Lesser Antilles. Contrib Mineral Petrol 172:98

Melnik O, Sparks R (2002) Dynamics of magma ascent and lava extrusion at Soufrière Hills Volcano, Montserrat. Geol Soc Lond Mem 21:153–171

Melnik O, Lyakhovsky V, Shapiro NM, Galina N, Bergal-Kuvikas O (2020) Deep long period volcanic earthquakes generated by degassing of volatile-rich basaltic magmas. Nat Commun 11:1–7

Métrich N, Rutherford M (1992) Experimental study of chlorine behavior in hydrous silicic melts. Geochim Cosmochim Acta 56:607–616

Métrich N, Rutherford MJ (1998) Low pressure crystallization paths of H 2 O-saturated basaltic-hawaiitic melts from Mt Etna: implications for open-system degassing of basaltic volcanoes. Geochim Cosmochim Acta 62:1195–1205

Métrich N, Wallace PJ (2008) Volatile abundances in basaltic magmas and their degassing paths tracked by melt inclusions. Rev Mineral Geochem 69:363–402

Métrich N, Bertagnini A, Landi P, Rosi M (2001) Crystallization driven by decompression and water loss at Stromboli volcano (Aeolian Islands, Italy). J Petrol 42:1471–1490

Métrich N, Bertagnini A, Landi P, Rosi M, Belhadj O (2005) Triggering mechanism at the origin of paroxysms at Stromboli (Aeolian Archipelago, Italy): the 5 April 2003 eruption. Geophysical Research Letters 32(10)

Métrich N, Bertagnini A, Di Muro A (2010) Conditions of magma storage, degassing and ascent at Stromboli: new insights into the volcano plumbing system with inferences on the eruptive dynamics. J Petrol 51:603–626

Métrich N, Allard P, Aiuppa A, Bani P, Bertagnini A, Shinohara H, Parello F, Di Muro A, Garaebiti E, Belhadj O (2011) Magma and volatile supply to post-collapse volcanism and block resurgence in Siwi Caldera (Tanna Island, Vanuatu Arc). J Petrol 52:1077–1105

Métrich N, Bertagnini A, Pistolesi M (2021) Paroxysms at Stromboli volcano (Italy): source, genesis and dynamics. Front Earth Sci 9:45

Molina I, Burgisser A, Oppenheimer C (2012) Numerical simulations of convection in crystal-bearing magmas: A case study of the magmatic system at Erebus, Antarctica. Journal of Geophysical Research: Solid Earth 117(B7)

Monaco C, Tapponnier P, Tortorici L, Gillot PY (1997) Late Quaternary slip rates on the Acireale-Piedimonte normal faults and tectonic origin of Mt. Etna (Sicily). Earth and Planetary Science Letters 147(1-4):125–39

Morgan JP, Ranero CR, Vannucchi P (2008) Intra-arc extension in Central America: links between plate motions, tectonics, volcanism, and geochemistry. Earth Planet Sci Lett 272:365–371

Moune S, Holtz F, Botcharnikov RE (2009) Sulphur solubility in andesitic to basaltic melts: implications for Hekla volcano. Contrib Mineral Petrol 157:691–707

Moussallam Y, Médard E, Georgeais G, Rose-Koga EF, Koga KT, Pelletier B, Bani P, Shreve TL, Grandin R, Boichu M (2021) How

to turn off a lava lake? A petrological investigation of the 2018 intra-caldera and submarine eruptions of Ambrym volcano. Bull Volcanol 83:1–19
Neuberg J, Luckett R, Baptie B, Olsen K (2000) Models of tremor and low-frequency earthquake swarms on Montserrat. J Volcanol Geotherm Res 101:83–104
Neuberg JW, Tuffen H, Collier L, Green D, Powell T, Dingwell D (2006) The trigger mechanism of low-frequency earthquakes on Montserrat. J Volcanol Geotherm Res 153:37–50
Nicholson E, Mather T, Pyle D, Odbert H, Christopher T (2013) Cyclical patterns in volcanic degassing revealed by SO2 flux timeseries analysis: an application to Soufrière Hills Volcano, Montserrat. Earth Planet Sci Lett 375:209–221
Okumura S, Nakamura M, Tsuchiyama A (2006) Shear-induced bubble coalescence in rhyolitic melts with low vesicularity. Geophysical research letters. 33(20)
Okumura S, Nakamura M, Tsuchiyama A, Nakano T, Uesugi K (2008) Evolution of bubble microstructure in sheared rhyolite: Formation of a channel-like bubble network. Journal of Geophysical Research: Solid Earth 113(B7)
Okumura S, Nakamura M, Uesugi K, Nakano T, Fujioka T (2013) Coupled effect of magma degassing and rheology on silicic volcanism. Earth and Planetary Science Letters. 362:163–70
Oppenheimer C, McGonigle A, Allard P, Wooster M, Tsanev V (2004) Sulfur, heat, and magma budget of Erta 'Ale lava lake, Ethiopia. Geology 32:509–512
Oppenheimer C, Bani P, Calkins J, Burton M, Sawyer G (2006) Rapid FTIR sensing of volcanic gases released by Strombolian explosions at Yasur volcano, Vanuatu. Appl Phys B Lasers Opt 85:453–460
Oppenheimer C, Lomakina AS, Kyle PR, Kingsbury NG, Boichu M (2009) Pulsatory magma supply to a phonolite lava lake. Earth Planet Sci Lett 284:392–398
Oppenheimer C, Moretti R, Kyle PR, Eschenbacher A, Lowenstern JB, Hervig RL, Dunbar NW (2011) Mantle to surface degassing of alkalic magmas at Erebus volcano. Antarctica. Earth and Planetary Science Letters. 306(3–4):261–71
Oppenheimer J, Rust A, Cashman K, Sandnes B (2015) Gas migration regimes and outgassing in particle-rich suspensions. Front Phys 3:60. https://doi.org/10.3389/fphy
Oppenheimer J, Capponi A, Cashman KV, Lane SJ, Rust AC, James MR (2020) Analogue experiments on the rise of large bubbles through a solids-rich suspension: a "weak plug" model for Strombolian eruptions. Earth and Planetary Science Letters. 531
Palma JL, Blake S, Calder ES (2011) Constraints on the rates of degassing and convection in basaltic open-vent volcanoes. Geochem Geophys Geosyst 12(11)
Parmigiani A, Faroughi S, Huber C, Bachmann O, Su Y (2016) Bubble accumulation and its role in the evolution of magma reservoirs in the upper crust. Nature 532:492–495
Parmigiani A, Degruyter W, Leclaire S, Huber C, Bachmann O (2017) The mechanics of shallow magma reservoir outgassing. Geochem Geophys Geosyst 18:2887–2905
Patrick MR, Orr T, Sutton A, Lev E, Thelen W, Fee D (2016) Shallowly driven fluctuations in lava lake outgassing (gas pistoning), Kīlauea Volcano. Earth Planet Sci Lett 433:326–338
Pelletier B, Calmant S, Pillet R (1998) Current tectonics of the Tonga-New Hebrides region. Earth and Planetary Science Letters. 164(1–2):263–76
Pérez W, Freundt A, Kutterolf S (2020) The basaltic plinian eruption of the~ 6 ka San Antonio Tephra and formation of the Masaya caldera, Nicaragua. J Volcanol Geotherm Res 401:106975
Pering TD, Ilanko T, Wilkes TC, England RA, Silcock SR, Stanger LR, Willmott JR, Bryant RG, McGonigle AJ (2019) A rapidly convecting lava lake at Masaya Volcano, Nicaragua. Front Earth Sci 6:241
Pering T, Liu E, Wood K, Wilkes T, Aiuppa A, Tamburello G, Bitetto M, Richardson T, McGonigle A (2020) Combined ground and aerial measurements resolve vent-specific gas fluxes from a multi-vent volcano. Nat Commun 11:1–11
Picard C, Monzier M, Eissen JP, Robin C (1994) Concomitant evolution of tectonic environment and magma geochemistry, Ambrym volcano (Vanuatu, New Hebrides arc). Geological Society, London, Special Publications. 81(1):135–54
Pichavant M, Di Carlo I, Le Gac Y, Rotolo SG, Scaillet B (2009) Experimental constraints on the deep magma feeding system at Stromboli volcano, Italy. J Petrol 50:601–624
Plank T, Balzer V, Carr M (2002) Nicaraguan volcanoes record paleoceanographic changes accompanying closure of the Panama gateway. Geology 30:1087–1090
Qin Z, Soldati A, Velazquez Santana LC, Rust AC, Suckale J, Cashman KV (2018) Slug stability in flaring geometries and ramifications for lava lake degassing. Journal of Geophysical Research: Solid. Earth 123:10,431–410,448
Ripepe M, Ciliberto S, Della Schiava M (2001) Time constraints for modeling source dynamics of volcanic explosions at Stromboli. J Geophys Res Solid Earth 106:8713–8727
Ripepe M, Delle Donne D, Genco R, Maggio G, Pistolesi M, Marchetti E, Lacanna G, Ulivieri G, Poggi P (2015) Volcano seismicity and ground deformation unveil the gravity-driven magma discharge dynamics of a volcanic eruption. Nat Commun 6:6998
Rodgers M, Roman DC, Geirsson H, LaFemina P, McNutt SR, Muñoz A, Tenorio V (2015) Stable and unstable phases of elevated seismic activity at the persistently restless Telica Volcano, Nicaragua. J Volcanol Geotherm Res 290:63–74
Roman DC, LaFemina PC, Bussard R, Stephens K, Wauthier C, Higgins M, Feineman M, Arellano S, de Moor JM, Avard G (2019) Mechanisms of unrest and eruption at persistently restless volcanoes: insights from the 2015 eruption of Telica Volcano, Nicaragua. Geochem Geophys Geosyst 20:4162–4183
Rose W, Rose Jr WI, Stoiber RE (1982) MalinconicoEruptive gas compositions and fluxes of explosive volcanoes: budget of S and Cl emitted from Fuego volcano, Guatemala R.S. Thorpe (Ed.), Andesites: Orogenic Andesites and Related Rocks, Wiley, New York, NY(1982), pp. 669–676
Rose WI, Palma JL, Delgado Granados H, Varley N (2013) Open-vent volcanism and related hazards: Overview. Understanding Open-Vent Volcanism and Related Hazards: Geological Society of America Special Paper 498
Rosi M, Bertagnini A, Landi P (2000) Onset of the persistent activity at Stromboli volcano (Italy). Bull Volcanol 62:294–300
Rosi M, Bertagnini A, Harris A, Pioli L, Pistolesi M, Ripepe M (2006) A case history of paroxysmal explosion at Stromboli: timing and dynamics of the April 5, 2003 event. Earth Planet Sci Lett 243:594–606
Rust A, Cashman K, Wallace P (2004) Magma degassing buffered by vapor flow through brecciated conduit margins. Geology 32:349–352
Ruth DC, Costa F, de Maisonneuve CB, Franco L, Cortés JA, Calder ES (2018) Crystal and melt inclusion timescales reveal the evolution of magma migration before eruption. Nat Commun 9:2657
Salerno G, Burton M, Oppenheimer C, Caltabiano T, Randazzo D, Bruno N, Longo V (2009) Three-years of SO 2 flux measurements of Mt. Etna using an automated UV scanner array: Comparison with conventional traverses and uncertainties in flux retrieval. J Volcanol Geotherm Res 183:76–83
Sanderson RW, Johnson J, Lees J (2010) Ultra-long period seismic signals and cyclic deflation coincident with eruptions at Santiaguito volcano, Guatemala. J Volcanol Geotherm Res 198:35–44

Sawyer GM, Carn SA, Tsanev VI, Oppenheimer C, Burton M (2008) Investigation into magma degassing at Nyiragongo volcano, Democratic Republic of the Congo. Geochemistry, Geophysics, Geosystems 9(2)

Scaillet B, Pichavant M (2003) Experimental constraints on volatile abundances in arc magmas and their implications for degassing processes. Geol Soc Lond, Spec Publ 213:23–52

Shapiro NM, Droznin D, Droznina SY, Senyukov S, Gusev A, Gordeev E (2017) Deep and shallow long-period volcanic seismicity linked by fluid-pressure transfer. Nat Geosci 10:442–445

Shinohara H (1994) Exsolution of immiscible vapor and liquid phases from a crystallizing silicate melt: Implications for chlorine and metal transport. Geochim Cosmochim Acta 58:5215–5221

Shinohara H (2008) Excess degassing from volcanoes and its role on eruptive and intrusive activity. Reviews of Geophysics 46(4)

Shinohara (2009) A missing link between volcanic degassing and experimental studies on chloride partitioning. Chem Geol 263:51–59

Shinohara H, Witter JB (2005) Volcanic gases emitted during mild Strombolian activity of Villarrica volcano, Chile. Geophysical Research Letters 32(20)

Shinohara H, Kazahaya K, Lowenstern JB (1995) Volatile transport in a convecting magma column: Implications for porphyry Mo mineralization. Geology 23:1091–1094

Shinohara H, Aiuppa A, Giudice G, Gurrieri S, Liuzzo M (2008) Variation of H2O/CO2 and CO2/SO2 ratios of volcanic gases discharged by continuous degassing of Mount Etna volcano, Italy. Journal of Geophysical Research: Solid Earth 113(B9)

Shinohara H, Ohminato T, Takeo M, Tsuji H, Kazahaya R (2015) Monitoring of volcanic gas composition at Asama volcano, Japan, during 2004–2014. J Volcanol Geotherm Res 303:199–208

Signorelli S, Carroll M (2002) Experimental study of Cl solubility in hydrous alkaline melts: constraints on the theoretical maximum amount of Cl in trachytic and phonolitic melts. Contrib Mineral Petrol 143:209–218

Spilliaert N, Métrich N, Allard P (2006) S–Cl–F degassing pattern of water-rich alkali basalt: modelling and relationship with eruption styles on Mount Etna volcano. Earth Planet Sci Lett 248:772–786

Steffke AM, Harris AJ, Burton M, Caltabiano T, Salerno GG (2011) Coupled use of COSPEC and satellite measurements to define the volumetric balance during effusive eruptions at Mt. Etna, Italy. J Volcanol Geotherm Res 205:47–53

Stevenson DS, Blake S (1998) Modelling the dynamics and thermodynamics of volcanic degassing. Bulletin of Volcanology. 60(4):307–17

Stix J (2007) Stability and instability of quiescently active volcanoes: the case of Masaya, Nicaragua. Geology 35:535–538

Stoiber RE, Williams SN, Huebert BJ (1986) Sulfur and halogen gases at Masaya caldera complex, Nicaragua: total flux and variations with time. J Geophys Res Solid Earth 91:12215–12231

Suckale J, Keller T, Cashman KV, Persson PO (2016) Flow-to-fracture transition in a volcanic mush plug may govern normal eruptions at Stromboli. Geophysical research letters. 43(23):12–071

Swanson D, Duffield W, Jackson D, Peterson D (1979) Chronolo ical narrative of the 1969-71 Mauna Ulu eruption of Kīlauea volcano. Hawaii US 8eol Surv Prof Pap 1056:55

Symonds RB, Rose WI, Bluth GJ, Gerlach TM (1994) Volcanic-gas studies; methods, results, and applications. Rev Mineral Geochem 30:1–66

Tamburello G, Aiuppa A, Kantzas E, McGonigle A, Ripepe M (2012) Passive vs. active degassing modes at an open-vent volcano (Stromboli, Italy). Earth Planet Sci Lett 359:106–116

Tamburello G, Pondrelli S, Chiodini G, Rouwet D (2018) Global-scale control of extensional tectonics on CO2 earth degassing. Nature communications. 9(1):1–9

Tattitch B, Chelle-Michou C, Blundy J, Loucks RR (2021) Chemical feedbacks during magma degassing control chlorine partitioning and metal extraction in volcanic arcs. Nat Commun 12:1–11

Tuffen H, Dingwell D (2005) Fault textures in volcanic conduits: evidence for seismic trigger mechanisms during silicic eruptions. Bull Volcanol 67:370–387

Vargas CA, Koulakov I, Jaupart C, Gladkov V, Gomez E, El Khrepy S, Al-Arifi N (2017) Breathing of the Nevado del Ruiz volcano reservoir, Colombia, inferred from repeated seismic tomography. Sci Rep 7:46094

Vergniolle S, Jaupart C (1986) Separated two-phase flow and basaltic eruptions. J Geophys Res Solid Earth 91:12842–12860

Vergniolle S, Métrich N (2021) Open-vent volcanoes: a preface to the special issue. Bull Volcanol 83:1–5

Wadge G, Voight B, Sparks R, Cole P, Loughlin S, Robertson R (2014) An overview of the eruption of Soufriere Hills Volcano, Montserrat from 2000 to 2010. Geol Soc Lond Mem 39:1–40

Wadge G, Kilbride BM, Edmonds M, Johnson R (2018) Persistent growth of a young andesite lava cone: Bagana volcano, Papua New Guinea. J Volcanol Geotherm Res 356:304–315

Waite GP, Nadeau PA, Lyons JJ (2013) Variability in eruption style and associated very long period events at Fuego volcano, Guatemala. Journal of Geophysical Research: Solid Earth. 118(4):1526–33

Walker JA, Williams SN, Kalamarides RI, Feigenson MD (1993) Shallow open-system evolution of basaltic magma beneath a subduction zone volcano: the Masaya Caldera Complex, Nicaragua. J Volcanol Geotherm Res 56:379–400

Wallace PJ (2005) Volatiles in subduction zone magmas: concentrations and fluxes based on melt inclusion and volcanic gas data. J Volcanol Geotherm Res 140:217–240

Wallace PJ, Gerlach TM (1994) Magmatic vapor source for sulfur dioxide released during volcanic eruptions: evidence from Mount Pinatubo. Science 265:497–499

Webster JD, Botcharnikov RE (2011) Distribution of sulfur between melt and fluid in SOHC-Cl-bearing magmatic systems at shallow crustal pressures and temperatures. Rev Mineral Geochem 73:247–283

Webster J, Kinzler R, Mathez E (1999) Chloride and water solubility in basalt and andesite melts and implications for magmatic degassing. Geochim Cosmochim Acta 63:729–738

Webster JD, Tappen CM, Mandeville CW (2009) Partitioning behavior of chlorine and fluorine in the system apatite–melt–fluid. II: Felsic silicate systems at 200 MPa. Geochim Cosmochim Acta 73:559–581

Webster JD, Goldoff BA, Flesch RN, Nadeau PA, Silbert ZW (2017) Hydroxyl, Cl, and F partitioning between high-silica rhyolitic melts-apatite-fluid (s) at 50–200 MPa and 700–1000 C. Am Mineral 102:61–74

Wech AG, Thelen WA, Thomas AM (2020) Deep long-period earthquakes generated by second boiling beneath Mauna Kea volcano. Science 368:775–779

Werner C, Fischer TP, Aiuppa A, Edmonds M, Cardellini C, Carn S, Chiodini G, Cottrell E, Burton M, Shinohara H, Allard P (2019) Carbon dioxide emissions from subaerial volcanic regions: two decades in review. In: Orcutt B, Daniel I, Dasgupta R (eds) Earth's Deep Carbon, Past to Present. Cambridge University Press

White SM, Crisp JA, Spera FJ (2006) Long-term volumetric eruption rates and magma budgets. Geochem Geophys Geosyst 7(3)

Williams SN (1983) Geology and eruptive mechanisms of Masaya Caldera complex. Dartmouth College, Nicaragua

Williams-Jones G, Rymer H, Rothery DA (2003) Gravity changes and passive SO 2 degassing at the Masaya caldera complex, Nicaragua. J Volcanol Geotherm Res 123:137–160

Witham F, Llewellin EW (2006) Stability of lava lakes. J Volcanol Geotherm Res 158:321–332

Witter JB, Kress VC, Delmelle P, Stix J (2004) Volatile degassing, petrology, and magma dynamics of the Villarrica Lava Lake, Southern Chile. J Volcanol Geotherm Res 134:303–337

Woitischek J, Woods AW, Edmonds M, Oppenheimer C, Aiuppa A, Pering TD, Ilanko T, D'Aleo R, Garaebiti E (2020) Strombolian eruptions and dynamics of magma degassing at Yasur Volcano (Vanuatu). Journal of Volcanology and Geothermal Research 398

Zajacz Z, Candela PA, Piccoli PM, Sanchez-Valle C (2012) The partitioning of sulfur and chlorine between andesite melts and magmatic volatiles and the exchange coefficients of major cations. Geochim Cosmochim Acta 89:81–101

Zuccarello L, Burton MR, Saccorotti G, Bean CJ, Patanè D (2013) The coupling between very long period seismic events, volcanic tremor, and degassing rates at Mount Etna volcano. J Geophys Res Solid Earth 118:4910–4921

Zurek J, Moune S, Williams-Jones G, Vigouroux N, Gauthier P-J (2019) Melt inclusion evidence for long term steady-state volcanism at Las Sierras-Masaya volcano, Nicaragua. J Volcanol Geotherm Res 378:16–28